Article

Current Biology

A new time tree of birds reveals the interplay between dispersal, geographic range size, and diversification

Graphical abstract

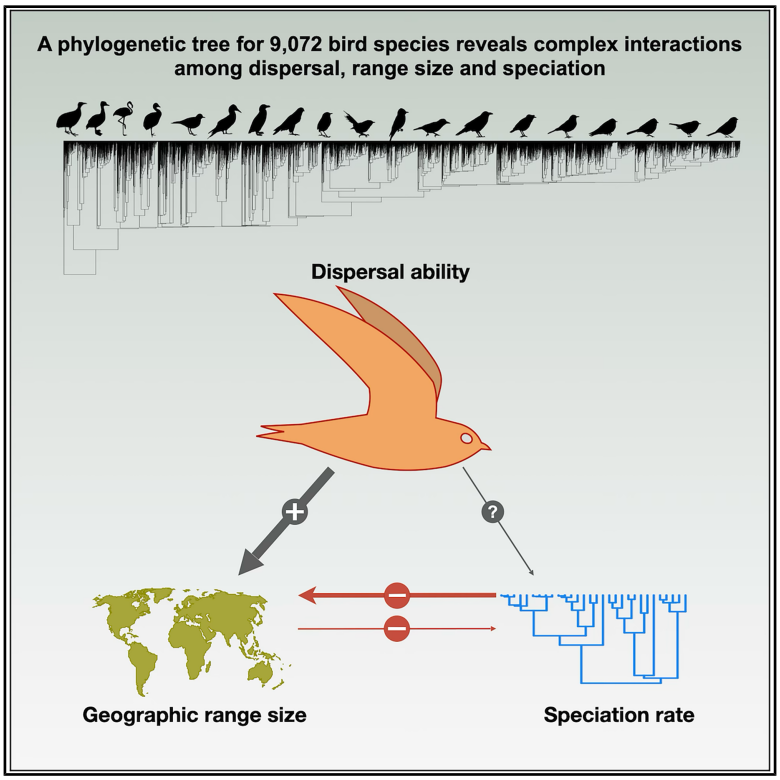

Authors

Santiago Claramunt, Catherine Sheard, Joseph W. Brown, ..., Michelle M. Su, Brian C. Weeks, Joseph A. Tobias

Correspondence

sclaramu@uno.edu

In brief

Flight may affect the dispersal and evolution of birds. Using a new evolutionary tree, Claramunt et al. find that efficient fliers have broader geographic ranges, and speciation reduces range size, but range size and flight efficiency have limited effects on speciation. Flight shapes bird diversity and evolution in complex ways.

Highlights

- We assembled a new time-scaled phylogenetic tree of the world's birds
- Dispersal ability increases range size but has minimal effects on speciation rates
- Small geographic ranges are associated with high speciation rates
- High speciation rates produce a reduction in geographic range size

Claramunt et al., 2025, Current Biology *35*, 1–13
August 18, 2025
https://doi.org/10.1016/j.cub.2025.07.004

CellPress

Current Biology

CellPress
OPEN ACCESS

Article

A new time tree of birds reveals the interplay between dispersal, geographic range size, and diversification

Santiago Claramunt,[1,2,9,*] Catherine Sheard,[3] Joseph W. Brown,[4] Gala Cortés-Ramírez,[5] Joel Cracraft,[6] Michelle M. Su,[1] Brian C. Weeks,[7] and Joseph A. Tobias[8]

[1]Department of Ecology and Evolutionary Biology, University of Toronto, Toronto, ON M5S 3G5, Canada
[2]Department of Biological Sciences, University of New Orleans, New Orleans, LA 70148, USA
[3]School of Biological Sciences, University of Aberdeen, Aberdeen AB24 3FX, UK
[4]Department of Natural History, Royal Ontario Museum, Toronto, ON M5S 2C6, Canada
[5]Facultad de Ciencias, Universidad Nacional Autónoma de México, Ciudad de México 04510, México
[6]Department of Ornithology, American Museum of Natural History, New York, NY 10024, USA
[7]School for Environment and Sustainability, University of Michigan, Ann Arbor, MI 48109, USA
[8]Department of Life Sciences, Imperial College London, London SW7 2AZ, UK
[9]Lead contact
*Correspondence: sclaramu@uno.edu
https://doi.org/10.1016/j.cub.2025.07.004

SUMMARY

The spatial and temporal dynamics of biodiversity are shaped by complex interactions among species characteristics and geographic processes. A key example is the effect of dispersal on geographical range expansion and gene flow, both of which may determine speciation rates. In this study, we constructed a time-calibrated phylogeny of over 9,000 bird species and leveraged extensive data on avian traits and spatial occurrence to explore the connections between dispersal, biogeography, and speciation. Phylogenetic path analyses and trait-dependent diversification models reveal that geographic range size is strongly associated with the hand-wing index, a proxy for wing aspect ratio related to flight efficiency and dispersal ability. By contrast, we found mixed evidence for the effect of dispersal on diversification rates: dispersive lineages show either slightly higher speciation rates or higher extinction rates. Our results therefore suggest that high dispersal ability increases range expansion and turnover, perhaps because dispersive lineages expand into islands or other geographically restricted environments and have lower population sizes. Our results highlight the nuanced and interconnected roles of dispersal and range size in shaping global patterns of avian diversification and biogeography and provide a richly sampled phylogenetic template for exploring a wide array of research questions in macroecology and macroevolution.

INTRODUCTION

The inter-relationships among dispersal, geographic range size, and speciation are complex yet fundamental to our understanding of macroecological and macroevolutionary patterns in biodiversity[1–4] (Figure 1). Dispersal influences geographic range size, as more dispersive species tend to occur across a wider area due to higher rates of range expansion and colonization.[5–7] Speciation, by contrast, typically results in the breakup of widespread ancestral geographic ranges into ranges constrained to a more limited geographical area.[8,9]

Dispersal is proposed to affect speciation in two contrasting ways. On one hand, higher rates of dispersal can reduce the chances of vicariant speciation if dispersing individuals boost rates of gene flow, inhibiting population differentiation.[10,11] On the other hand, the capacity to cross geographical barriers and colonize new regions introduces a potential positive effect of dispersal on peripatric speciation.[2,4,12] This dual effect of dispersal on speciation may result in a trade-off whereby speciation rates peak at intermediate levels of dispersal.[13–15] Poor dispersers may remain as isolated geographic endemics with little chance of further speciation, while the most dispersive species would undergo little genetic differentiation across their extensive geographic ranges owing to the homogenizing effect of gene flow. Only species with intermediate dispersal capabilities would experience cycles of colonization and isolation that maximize the chances of speciation.[13–15] Recent theoretical studies based on population genetic models in a two-island setting[16] and spatial-explicit individual-based simulations[17] demonstrated the plausibility of the intermediate dispersal model under basic conditions, suggesting that the pattern could be widespread in nature. However, previous analyses that have attempted to test this speciation cycle model were restricted to narrow taxonomic groups or geographic regions,[13,18,19] primarily because standardized estimates of dispersal, range size, and rates of speciation are generally not available at sufficient scale.

In this study, we use global datasets of biogeography and functional traits[20] together with a newly assembled

Please cite this article in press as: Claramunt et al., A new time tree of birds reveals the interplay between dispersal, geographic range size, and diversification, Current Biology (2025), https://doi.org/10.1016/j.cub.2025.07.004

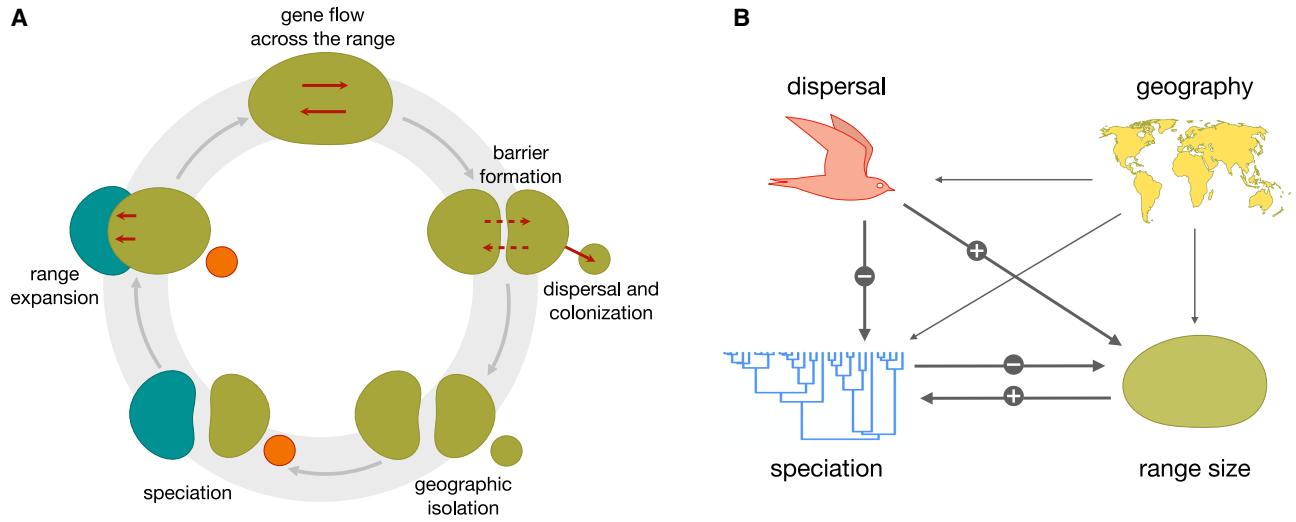

Figure 1. Hypothetical interactions between dispersal, geography, and speciation

(A) Conceptual representation of the speciation cycle in the context of organismal dispersal and geographical dynamics. Colored shapes depict geographical ranges, and red arrows indicate dispersal driving gene flow within or between ranges and colonization of new ranges. The formation of new species can be driven by vicariance (teal) or founder events (orange).

(B) Predicted cause-effect interactions among dispersal, geographic range size, and speciation based on the conceptual model.

time-calibrated phylogeny to investigate the interplay between dispersal, range size, and speciation rates in birds. Capitalizing on rapid growth of genomic resources and high-quality molecular phylogenies, we assembled a new time tree of birds to generate updated estimates of diversification rates. To estimate dispersal ability, we used two classic morphological proxies: body mass and hand-wing index (HWI). Body mass influences dispersal because large animals tend to have increased locomotor capacity, move over longer distances, and are more resilient during transit and establishment.[21–23] HWI is a proxy of wing aspect ratio known to predict dispersal ability and gap-crossing potential in birds because of its association with flight efficiency.[24–26] We also incorporated two geographic factors: latitude of the geographical range (correlated with temperature and seasonality) and the association with islands (linked to constraints on range size and dispersal). We then analyzed interactions among these factors using phylogenetic comparative methods and diversification models[27,28] to assess key predictions of the speciation cycle (Figure 1).

RESULTS

An expanded and updated time tree of birds

We assembled a time-scaled phylogeny of 9,072 bird species, spanning over 80% of avian species diversity, including recently extinct species (Figure 2; STAR Methods). This sample expands the size of earlier trees based on DNA supermatrices[29,30] by an additional 2,402–2,358 species with molecular data (35%–36% more). Topological accuracy is also expected to be higher in this new tree compared with previous trees assembled using stochastic addition of missing taxa.[30,31] Some relationships among major groups are better resolved, including the position of Tinamidae within[32] rather than sister[30] to ratites. Estimated divergence times generally agree with recent estimates using whole genomes and quantitatively derived calibration priors.[33–35] For example, the split between Anseriformes and Galliformes is estimated at 67.7 Ma, and the beginning of the rapid radiation of Neoaves at 70.6 Ma, near the Cretaceous-Paleogene boundary, in alignment with 68.2 and 67.4 Ma, respectively, as reported in the whole-genome time tree.[35] Other bird phylogenies generally estimate older ages for these two events.[30,31] Perhaps most importantly, all branch lengths in our tree are derived from DNA sequence data, with no use of interpolation or averaging, unlike other comprehensive avian time trees.[30,31] This provides a solid phylogenetic template suited for the analyses of diversification rates.

New speciation rate estimates for birds

We estimated lineage-specific speciation rates across the new time tree using the ClaDS2 method[38] (Figure 2B). Estimates spanned three orders of magnitude, from as low as 0.014 lineages/Ma in the Greater Rhea (*Rhea americana*) lineage to as high as 2.98 lineages/Ma in the Tawny-bellied Seedeater (*Sporophila hypoxantha*) lineage (Figure 2B). Other lineages that showed very low (<0.02 Ma^{-1}) speciation rates included large ratites (*Casuarius*, *Dromaius*, and *Struthio*), the Sunbittern (*Eurypyga helias*), the Kagu (*Rhynochetos jubatus*), the Brown Mesite (*Mesitornis unicolor*), and some finfoots (Heliornithidae), wood hoopoes (Phoeniculidae), ground cuckoos (*Dromococcyx* and *Tapera*, Cuculidae), and darters (Anhingidae). At the other extreme, lineages producing more than one species per million years can be found among capuchino seedeaters (*Sporophila*, Thraupidae), indigobirds (*Vidua*, Viduidae), ground finches (*Geospiza*, Thraupidae), white-eyes (*Zosterops*, Zosteropidae), *Pyrrhura* parakeets and *Trichoglossus* lorikeets (Psittaciformes), *Anas* ducks (Anatidae), and *Larus* gulls (Laridae). These groups can be considered the true "great speciators" among birds.

Please cite this article in press as: Claramunt et al., A new time tree of birds reveals the interplay between dispersal, geographic range size, and diversification, Current Biology (2025), https://doi.org/10.1016/j.cub.2025.07.004

CellPress
OPEN ACCESS

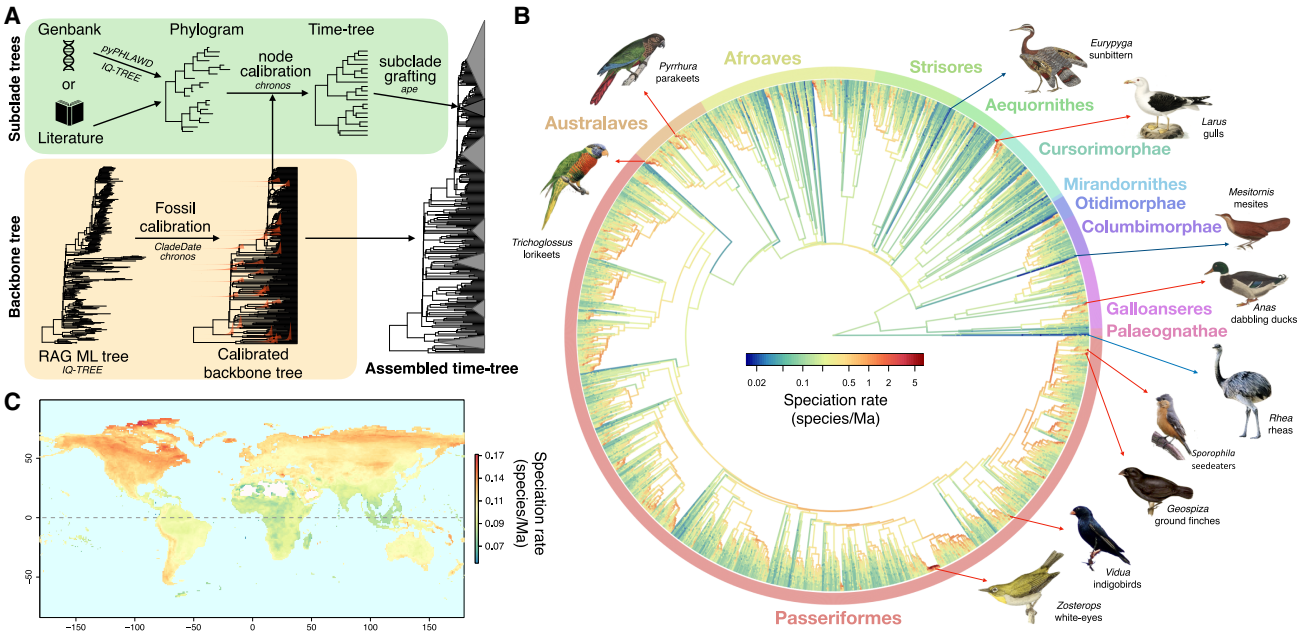

Figure 2. A new time tree for the world's birds

(A) Visual summary of methods used to assemble a composite time-calibrated tree of birds. A "backbone" tree of avian families was inferred by maximum likelihood (ML) using sequences of recombination activating genes 1 and 2, which was then time-scaled using 33 calibration densities (red) derived empirically from the fossil record. Species-level phylogenies of 47 subclades were obtained from previous studies or inferred using GenBank mining algorithms (phPHLAWD) and ML inference and then time-scaled using node age information from the calibrated backbone tree. Subclade trees were then grafted into the backbone tree to assemble the final tree of 9,072 bird species, representing 80% of all bird species (35% more than previous sequence-based global bird trees). Key software and algorithms are stated in italics.

(B) Time-calibrated phylogeny of the world's birds showing lineage-specific speciation rates estimated using the ClaDS2 method.[36] The colored circle marks major clades following Braun et al.[37] except that, for simplicity, Aequornithes includes Phaethontimorphae, Opisthocomiformes is included in Cursorimorphae, and Passeriformes is separated from the more inclusive Australaves. Illustrations represent clades that experienced the lowest (blue) and the highest (red) rates of speciation. The latter can be considered "the great speciators" of the avian world. Bird images counterclockwise from the rightmost point: *Rhea americana* (Eric Kilby, CC BY-SA 2.0), *Anas platyrhynchos* (Rvalette, CC BY-SA 3.0), *Mesitornis unicolor* (M.A.P.C. Des Murs, public domain), *Larus fuscus* (Rawpixel, CC BY-SA 4.0), *Eurypyga helias* (Rvalette, CC BY-SA 3.0), *Pyrrhura lucianii* (F.-L. Laporte, public domain), *Trichoglossus haematodus* (J. Smit, public domain), *Zosterops maderaspatanus* (J.G. Keulemans, public domain), *Vidua chalybeata* (B. Dupont, CC BY-SA 2.0), *Geospiza fortis* (J. Gould, public domain), and *Sporophila hypoxantha* (H. Bottai, CC BY-SA 3.0), all sourced from Wikimedia Commons.

(C) Global map of average speciation rates in birds. Lineage-specific speciation rates estimated using the new time tree and the ClaDS2 algorithm were projected on the species geographic range map (from BirdLife International 2019.1) and averaged at the 1° × 1° scale. Squares with fewer than 15 species were omitted (gray).

Geographic patterns of variation in lineage-specific speciation rates show higher average rates in colder regions both at high latitudes and high elevations, including the tundra and boreal forest of the Holarctic, the Patagonian and central Asian steppes, and the high Andes of South America (Figure 2C). North America and Oceania also show high speciation rates, whereas the Paleotropics (Afrotropics and tropical South and Southeast Asia) show low average speciation rates.

Phylogenetic signal and covariation

Most factors analyzed, with the exception of speciation rates, showed moderate to high levels of phylogenetic inertia, as estimated from a *lambda* model of trait evolution (Table S1). We found high phylogenetic signal in body mass (log-transformed, *lambda* = 0.99) and HWI (0.96). Absolute latitude had slightly lower levels of phylogenetic signal (0.91), and geographic range size (log-transformed) had the lowest levels (0.68), as expected given that range size does not evolve in a Brownian fashion.[9,39] Speciation rates were best explained by a speciational model of trait evolution in which the amount of change is not proportional to time but proportional to the number of speciation events along lineages. Bivariate relationships do not reveal strong linear associations among factors (Figure 3). Consistent with the phylogenetic signal analysis, values for body mass and HWI were taxonomically clustered, with major clades occupying distinct portions of morphospace (Figure 3).

Interactions among macroevolutionary and macroecological factors

To test hypotheses about causal effects among dispersal traits and geographic factors in the speciation cycle, we conducted a phylogenetic path analysis. The results revealed substantial differences in effects (Figure 4). The HWI had a strong positive effect on geographic range size, as reported previously,[40] and a small but statistically significant positive effect on speciation rates. Body mass, by contrast, had a negative effect on range size and no effect on speciation rates. We found that speciation reduces geographic range size, in line with predictions.

Please cite this article in press as: Claramunt et al., A new time tree of birds reveals the interplay between dispersal, geographic range size, and diversification, Current Biology (2025), https://doi.org/10.1016/j.cub.2025.07.004

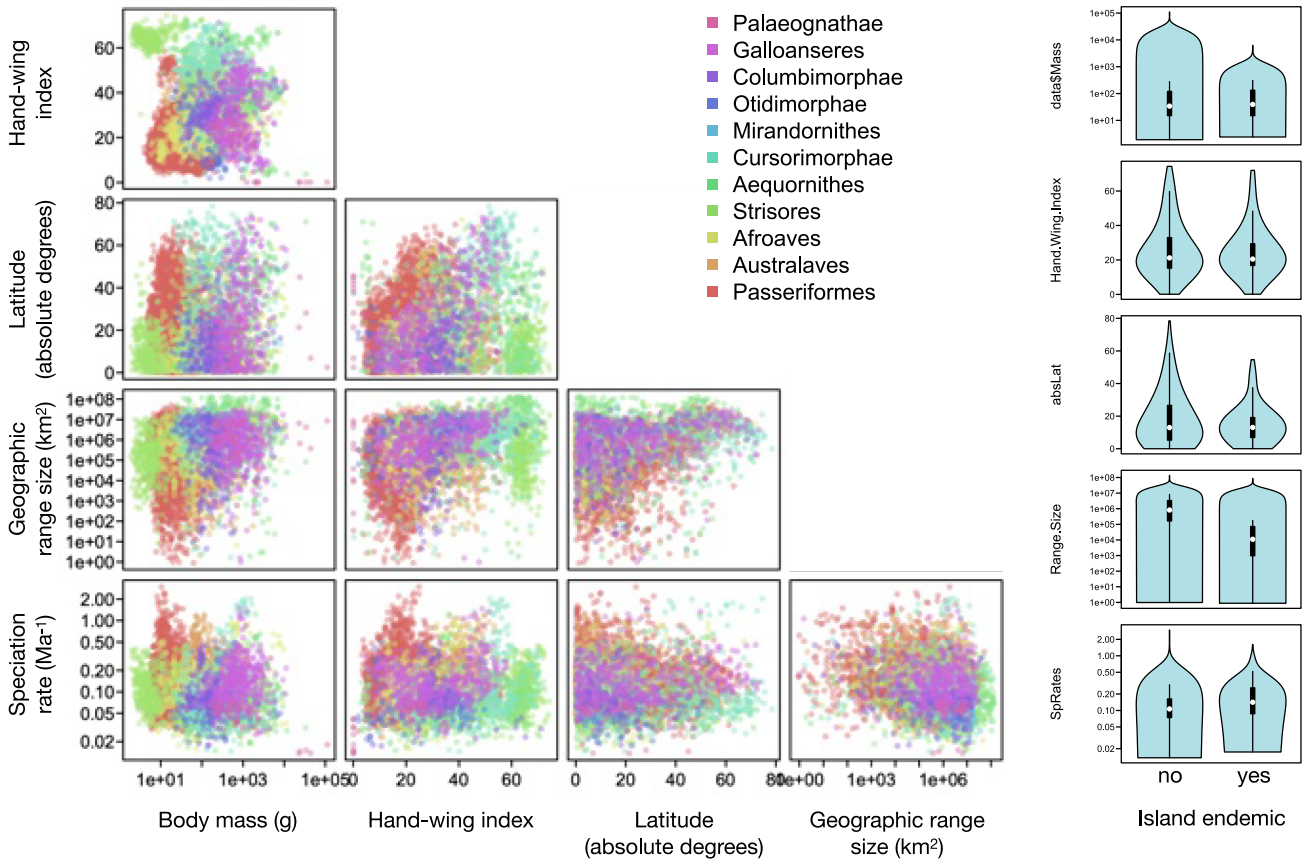

Figure 3. Covariation among dispersal, geography, and speciation rates in birds

Bivariate relationships among dispersal proxies (HWI and body mass), geographic settings (latitude and island dwelling), geographic range size, and speciation rates in 8,740 species of birds. Colors representing major avian clades follow the schema in Figure 2.

However, we found no significant evidence for an effect of range size on speciation rates (Figure 4; Table S2), although this relationship is inherently difficult to detect (see discussion).

Geographic covariates were also influential: higher latitudes were associated with higher HWI, greater body mass, and larger range size, in agreement with recent macroecological analyses,[40] Bergmann's rule,[41] and Rapoport's rule,[42] respectively (Figure 4; Table S2). Island dwelling was associated with smaller range sizes, lower HWI, and higher speciation rates. Overall, the strongest effects were on geographic range size, whereas effects on speciation rates were of small magnitude (<0.05) and often not statistically significant (Figure 4; Table S2). A sensitivity analysis using an alternative definition of island dwelling, in which we used the proportion of the species distribution that occurs on islands smaller than 2,000 km^2, produced remarkably similar results except for a general attenuation of the effect of island distribution (Figure S1).

To provide a preliminary assessment of variation in clade-specific mechanisms, we re-ran analyses on two phenotypically and ecologically different subclades: (1) the order Passeriformes, composed of mostly small non-aquatic species, and (2) a clade of larger, predominantly aquatic birds, including shorebirds, gulls, and terns (Charadriiformes); rails and cranes (Gruiformes); and penguins, petrels, storks, pelicans, cormorants, herons, and allies (Aequornithes). The results for Passeriformes were very similar to those found across all birds, except for a reduction in the effects of the HWI on range size and speciation, the latter no longer significant (Figure S1). Waterbirds showed decreased effects of HWI and body mass on range size to the extent that the relationships were no longer statistically significant (Figure S2). Perhaps most notably, body mass had a moderate positive effect on speciation rates in waterbirds. Other effects remained similar to those found across all birds.

How dispersal and biogeography influence diversification rates

To assess in more detail how dispersal traits and geographic factors influence speciation and extinction, we used quantitative-state speciation and extinction (QuaSSE) models.[43] While path analysis only considers linear relationships among factors, QuaSSE considers different functional relationships between quantitative traits and rates of speciation and extinction, allowing for an evaluation of the intermediate dispersal model (STAR Methods). We found no evidence that intermediate dispersal promotes speciation using either of our dispersal proxies (body mass and HWI). Speciation rates increased with body mass (Figure 5A), but extinction rates increased even more rapidly so that net diversification rates peaked at 20 g and then declined

Please cite this article in press as: Claramunt et al., A new time tree of birds reveals the interplay between dispersal, geographic range size, and diversification, Current Biology (2025), https://doi.org/10.1016/j.cub.2025.07.004

CellPress
OPEN ACCESS

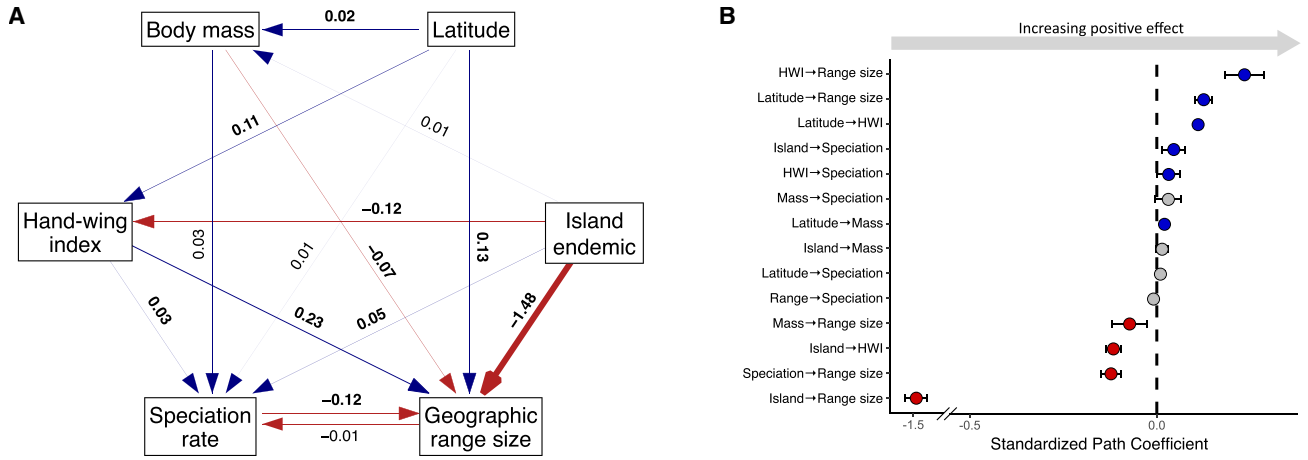

Figure 4. Phylogenetic path analysis of macroecological and macroevolutionary factors in birds

(A) Graph showing paths (arrows) and associated path coefficients representing the direction and strength of the effects of one factor on another. Arrow thickness is proportional to the magnitude of the effect (path coefficient), and arrow color indicates the direction of the effect: positive (blue) or negative (red). Body mass, geographic range size, and speciation rates were log-transformed. Latitude refers to absolute latitude.

(B) Standardized path coefficients with confidence intervals for each path. "HWI" is the hand-wing index, a proxy for flight efficiency and dispersal ability. "Range size" is the geographic range size. The dot color indicates the direction and statistical significance of the effect based on the confidence interval: positive (blue), negative (red), or statistically not different from zero (gray) (Table S2).

See also Figures S1 and S2 and Table S2.

for larger birds (Figure 5A). HWI did not influence speciation rates, but extinction rates increased for HWI >25, bringing the relative extinction rate to 0.68 and halving the net diversification rate (Figure 5B). Diversification rates were essentially constant across latitudes.

The effect of islands was evaluated using hidden-state speciation and extinction (HiSSE) models, which examine the effect of binary traits on diversification rates while allowing rates to be affected by additional unmeasured ("hidden") states.[44] Speciation rates increased from 0.14 Ma^{-1} for continental species to 0.27 Ma^{-1} for island endemics (Figure 5D). However, extinction also increased from 0 to 0.22 Ma^{-1} on islands, resulting in a decrease in the net rate of diversification (Figure 5D). When we re-ran these analyses with a narrower definition of island dwelling, we found again that extinction rates increased even higher for species occurring on very small islands (<2,000 km^2), resulting in negative net diversification rates (Figure S3). Finally, both speciation and extinction changed dramatically with geographic range size. Speciation rates were high (0.31 lineages/Ma) for range sizes <1 million km^2 but low (0.02) for larger ranges. Extinction was fairly low for range sizes >22,000 km^2 but jumped to 0.5 lineages/Ma in smaller ranges, again resulting in negative net diversification rates (Figure 5E). Only lineages with intermediate range sizes had high net diversification rates (Figure 5E).

Because QuaSSE models are prone to false positives,[45] we ran sensitivity analyses using two more conservative techniques. First, we used HiSSE models on discretized versions of our continuous factors. For body mass, HWI, and latitude, character-independent diversification (CID) models were superior (Table S7). For geographic range size, we used a model that takes into account the splitting of geographic ranges during speciation, designed to detect the effect of speciation on range size while avoiding the cofounding association between speciation and small ranges that are the result, not the cause, of high speciation rates.[39] This model was better than the corresponding character-independent models and suggested a reduction in speciation rates for widespread lineages, in line with the QuaSSE results, although the magnitude of the reduction was small (0.20–0.18 Ma^{-1}; Figure S4). Second, we evaluated the statistical significance of linear correlations between traits and species-specific speciation rates using the ES-sim method, a semi-parametric method based on trait evolution simulations.[45] Using our ClaDS estimates of species-specific speciation rates and fast Brownian motion simulations, we found statistically significant linear effects on speciation for geographic range size and percent of island distribution (Figure S5).

DISCUSSION

We present the first comprehensive study of the interplay between dispersal ability, geographic range size, and speciation rates in a major vertebrate radiation. We assembled a phylogeny of 9,072 bird species using a fossil-calibrated backbone tree and 47 species-level phylogenies that provide an improved framework for analyzing diversification rates in birds. The results provide strong evidence for the effect of dispersal on geographic range size in birds, concordant with previous studies.[5,40,46] In particular, we found a strong positive effect of HWI on geographic range size. Because of its direct relationship with wing aspect ratio, HWI reflects the aerodynamic efficiency of flight[47–49] and has been shown to predict natal dispersal distances,[24,26,50] as well as the ability to cross fragmented landscapes[51] and other dispersal barriers.[13,52] Therefore, our results confirm that locomotor capacity, and flight efficiency in particular, has a strong effect on range expansion and ultimately range size in birds.

By contrast, the effect of body mass on geographic range size was not only small but negative (Figure 5). This contrasts with the

Please cite this article in press as: Claramunt et al., A new time tree of birds reveals the interplay between dispersal, geographic range size, and diversification, Current Biology (2025), https://doi.org/10.1016/j.cub.2025.07.004

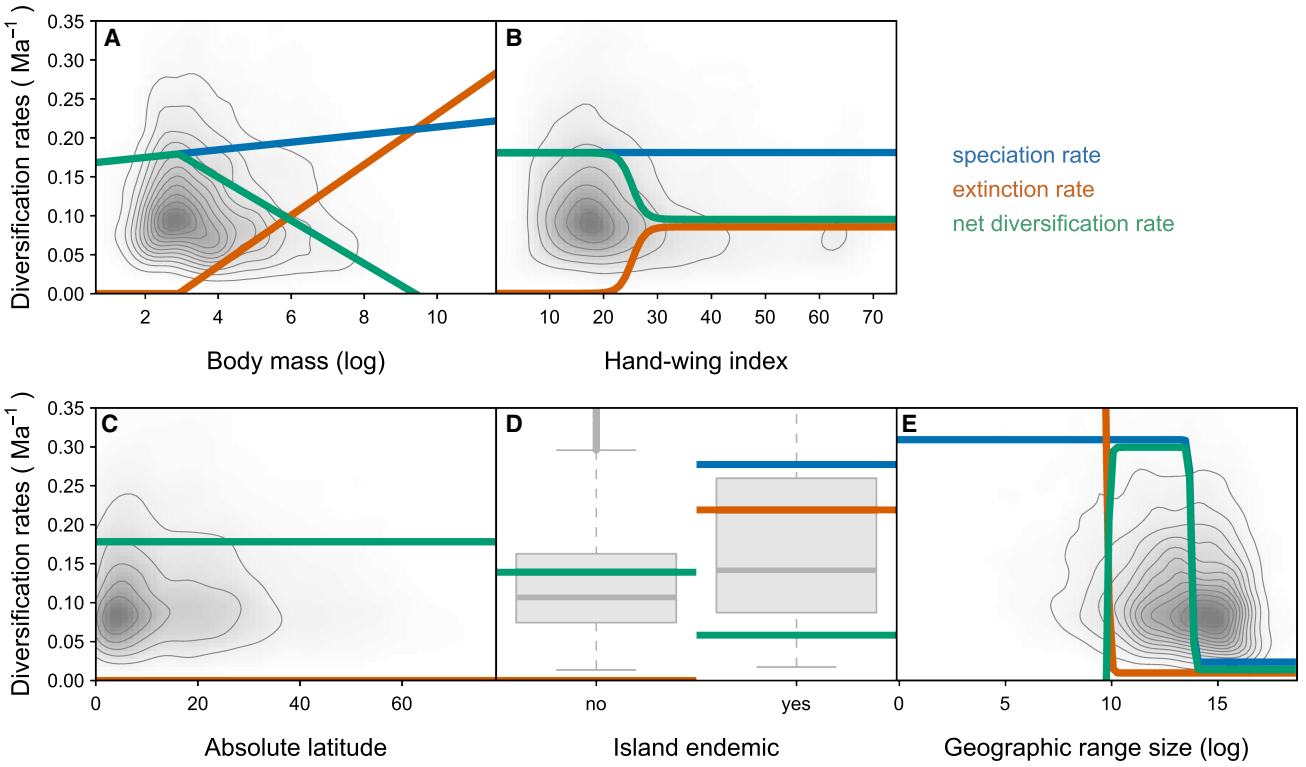

Figure 5. Dispersal and geographic attributes affect bird diversification rates

Relationship between species traits—body mass (A) and hand-wing index (B)—and geographic attributes—absolute latitude (C), island dwelling (D), and geographic range size (E)—and diversification rates in the world's birds. Lines show predictions from quantitative-state speciation and extinction (QuaSSE) models for continuous traits and hidden-state speciation and extinction (HiSSE) models for island dwelling: speciation rates (blue), extinction rates (orange), and net diversification rates (green) calculated as speciation rate – extinction rate. The best model for each trait was identified using model selection techniques (Tables S3–S6). Shaded contour lines show the density of species in the trait-speciation rate (ClaDS) scatterplots from Figure 2.
See also Figures S3–S5 and Tables S3–S7.

classic macroecological expectation that body mass and range size will be positively related as a result of fewer large species with small ranges, resulting in a triangular pattern in a log-log plot.[1,53] While the triangular pattern is apparent in our data (Figure 3), we still found a negative effect of body mass on range size (Figure 4). We suggest that the triangular pattern may be produced by the independent effects of (1) the low number of large species and (2) a left-skewed distribution of range sizes. The gradual scarcity of larger species is reflected in the right-skew distribution of log-transformed body masses,[53] a pervasive pattern in macroecology that could be explained by higher extinction risk among larger species.[54] Once log-transformed, geographic range sizes tend to show a left skew,[8] a pattern that may be produced by the effect of speciation splitting ancestral ranges[9] (see also next section). The combination of left-skewed log-range sizes and right-skewed log-body masses alone can generate a triangular pattern. As a demonstration, we produced a plot by randomizing body masses across species, and we recovered a strong triangular pattern (Figure 6). Therefore, it is plausible that a combination of extinction reducing the number of large species and speciation reducing range size, acting independently, creates the triangular pattern without the need for body mass to influence range size or other more complex explanations.[1,27,55]

Range size as a consequence, not a driver of speciation

We found a negative effect of speciation on geographic range size, as expected given the predominance of a vicariant mode of speciation in birds, whereby the speciation process splits ancestral ranges, resulting in smaller ranges for daughter species.[8,9] By contrast, we did not find that larger geographic ranges result in higher speciation rates. Path analysis did not detect a significant effect of geographic range size on speciation rates, and trait-dependent diversification modeling indicated lower speciation rates among widespread lineages. On the other hand, we detected a spike in extinction rates for lineages with very small ranges, resulting in negative net rates of diversification. This is expected due to elevated extinction risk in small populations due to ongoing decreasing trends, demographic stochasticity, genetic meltdown, or Allee effects.

Assessing the effect of geographic range size on speciation is difficult because the process of speciation links speciation and geographic range evolution in a way that is not well captured with either path analysis or QuaSSE models. In particular, because speciation rates are based on information from the past (phylogenetic history) and geographic range sizes are assessed in the present, causes and effects may be difficult to disentangle. For example, recent allopatric speciation events

Please cite this article in press as: Claramunt et al., A new time tree of birds reveals the interplay between dispersal, geographic range size, and diversification, Current Biology (2025), https://doi.org/10.1016/j.cub.2025.07.004

CellPress
OPEN ACCESS

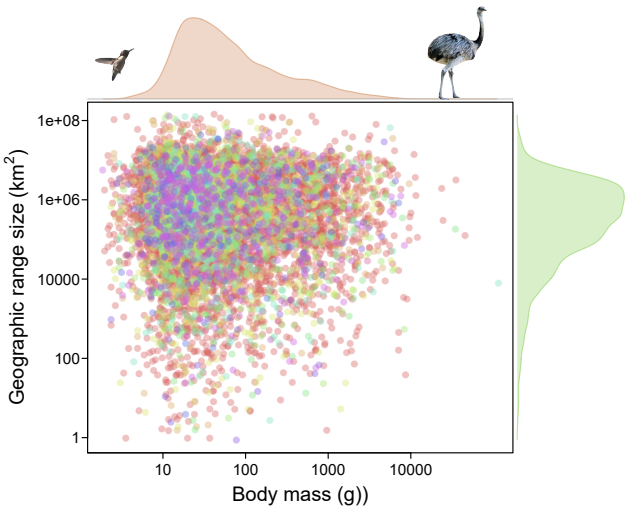

Figure 6. Triangular relationship between body mass and range size
The triangular pattern in the relationship between body mass and geographic range size (both in logarithmic scale) was recreated with a randomized sample in which the original distributions of both body mass (top) and range size (left) were preserved but the species identity was scrambled. Therefore, this widespread pattern need not necessarily arise from a mechanistic interaction between body mass and range size and may instead be an effect of the scarcity of large-bodied birds and very small distributions. Illustrated birds are the smallest bird, the Bee Hummingbird (*Mellisuga helenae*, modified from a photo by E. Chernetsova, CC BY 2.0 via Wikimedia Commons), and one of the largest birds, the Greater Rhea (*Rhea americana*, modified from a photo by E. Kilby, CC BY-SA 2.0, via Wikimedia Commons, not at scale).

resulting in multiple modern-day lineages with small geographical ranges may be interpreted by linear modeling as an effect of small geographic ranges stimulating speciation.[39] QuaSSE models provide more explicit tests of cause-effect relationships but assume a Brownian model of trait evolution, which does not capture the abrupt and unidirectional shifts in range size associated with speciation events. Nonetheless, we also detected lower speciation rates in lineages with large range sizes using an alternative method[39] that explicitly accounts for the reduction of ranges produced by speciation, albeit at the cost of modeling range size as a discrete binary trait (small versus large).

Another limitation of current trait-dependent diversification models is that they consider a single factor, whereas diversification dynamics are typically shaped by a variety of factors, leading to multiple indirect effects that can confound results. For example, higher speciation rates among narrowly distributed lineages (Figure 5) may reflect occurrence on islands, so high speciation rates may arise due to isolation, not range size. Similarly, lower speciation rates among some widespread lineages may reflect high dispersal ability, which promotes gene flow across geographic barriers, impeding speciation. We suggest that the effect of range size on speciation rates varies according to species traits and that speciation cycles can proceed along different pathways depending on geographic context.

The effect of dispersal ability on speciation is complex

At a global scale, we found no consistent effect of dispersal ability on diversification rates. Flightless (ratites and penguins) and some near-flightless species (ground cuckoos, lyrebirds, and rockfowls) show low speciation rates, but other near-flightless groups, such as *Scytalopus* tapaculos, show relatively high speciation rates (see also Cadena et al.[56]). In addition, lineages with more efficient flight were not consistently associated with lower speciation rates (Figure 3). State-dependent models (QuaSSE and HiSSE) did not detect effects of wing shape on speciation rates, while path analysis detected slight but significant increases in speciation among lineages with stronger flight capacity (Figures 4 and 5). These results suggest that, if anything, higher dispersal ability stimulates speciation, in agreement with some previous studies[2,4,12,57] but in contrast with others that have shown negative relationships between dispersal and diversification.[13,18]

As with other mechanisms investigated here, the relationship between dispersal ability and diversification may be affected by sampling biases and geographical context.[4,13] In continuous landscapes with high connectivity, even low levels of dispersal can inhibit speciation, whereas in fragmented landscapes, dispersal may stimulate speciation.[13,17] For example, ovenbirds and woodcreepers (Furnariidae) that have diversified mostly within the South American continent show a negative relationship between dispersal ability and speciation rates.[13] By contrast, honeyeaters (Meliphagidae) that diversified across Australasian archipelagos show a positive relationship between dispersal ability and speciation rates.[19]

Overall, the weak positive effects of dispersal on speciation at a global scale may be due to an increase in diversification related to colonization of new continents or oceanic archipelagos facilitated by high dispersal ability,[19,58,59] an effect that may not be apparent at smaller regional or taxonomic scales.[60–62] Birds that have colonized the most isolated islands, in particular, tend to have more efficient flight capabilities[6] but subsequently may experience elevated levels of isolation and evolution toward reduced flight capacity,[63] two factors that may stimulate speciation.[64] For example, oceanic birds such as albatrosses and petrels that breed in isolated oceanic islands can travel long distances but are highly philopatric, and their highly efficient flight may not compensate for the isolation of their breeding grounds, leading to low levels of gene flow across populations. An additional pathway to speciation for lineages with efficient flight is via migratory drop-offs, in which migratory birds establish a breeding population in their wintering ground and then become isolated from the original breeding population.[65,66]

In addition to the effect of speciation after colonization, we propose an alternative explanation for why high dispersal ability may be associated with high speciation even in vicariant speciation scenarios. Recent comparative studies in birds suggest that more dispersive species tend to live at lower densities and have smaller population sizes.[50,67] Among British and North American birds, there is a negative correlation between population size and both natal dispersal distances and the HWI,[24,50] and dispersal ability tends to be higher in dry and cold regions,[40] where bird population densities are lower.[68] Lower population levels may increase extinction rates of these lineages and potentially increase speciation rates because the effect of gene flow on population differentiation depends on the absolute number of migrants.[69,70] Thus, even though per capita dispersal rates may be high for highly dispersive species, levels of gene flow may be relatively low due to lower population size. This

effect may explain why population genetic studies have not consistently found the expected negative relationship between dispersal ability and genetic differentiation[71–73] and why rates of speciation remain relatively stable across a wide range of dispersal capabilities (Figures 3 and 5).

Geographic drivers of diversification

We detected a strong effect of island dwelling on diversification (Figures 4 and 5D). Although the effect was of small magnitude in the path analysis (0.02), trait-dependent diversification modeling revealed a substantial increase in both speciation and extinction in island birds. Because the increase in extinction rates was of greater magnitude, island birds experienced higher speciation but lower net diversification rates (Figure 5D). This result is consistent with the widespread heightened vulnerability to extinction among island birds due to their sensitivity to anthropogenic and natural threats arising from a range of factors, such as small population sizes, population isolation, and vulnerability to invasive predators, competitors, and parasites.[64,74–76]

By contrast, latitude did not affect diversification rates. Across our different modeling techniques, speciation (and extinction) rates remained constant across latitudes (Figures 4 and 5D). These results broadly align with recent studies showing minimal effects of latitude on speciation rates.[77–79] The projection of lineage-specific speciation rates on a map shows the average speciation rate increasing toward high latitudes (Figure 2), but the pattern is more complex than a latitudinal trend, potentially resulting from other factors, such as wing shape and dispersal ability,[40] that covary with latitude and may affect speciation rates.

Overall, the effects of dispersal and geographic factors on speciation rates were small (Figure 4). One possibility is that these factors, although influential, are not the main drivers of speciation. Speciation may instead be driven by abiotic processes controlling the dynamics of range expansion and the formation of geographic barriers that trigger speciation.[80–82] For example, the signature of dispersal traits could be erased by climatic events triggering habitat expansion and the passive transportation of species from one region to another or across a previous barrier. This view is supported by mounting evidence highlighting the effect of habitat types, habitat distribution, and the dynamism of geographic barriers on population genetic differentiation and speciation.[71,81,83–86]

Alternatively, dispersal and geography may be important factors regulating speciation, but our estimates of speciation rates may not be sufficiently accurate to recover these relationships. Although the ClaDS2 algorithm accounts for missing species, it only accounts for extinction indirectly by assuming a constant turnover rate.[36] Turnover may be constant if rates of speciation and extinction are positively correlated, as often proposed.[87,88] Indeed, such a correlation is predicted under the classic model of speciation cycles, as speciation-induced subdivision of ancestral geographic ranges results in smaller populations that are more prone to extinction, producing a negative feedback,[4,82,87] and it also emerges in spatially explicit individual-based simulations of diversification.[17] However, turnover rates may not be constant across birds, as shown in our QuaSSE models (Figure 5). This highlights the need to estimate extinction rates independently to assess whether they are influenced by dispersal traits or biogeography and to study how extinction may shape variation in body size and range size across species, potentially leading to some classic macroecological and macroevolutionary patterns.[1,27,54,77] Finally, speciation rate estimates may be affected by errors or biases in the phylogenetic tree. In particular, estimates of speciation and extinction rates depend heavily on the length of the terminal branches of phylogenies, which are often subject to biases due to sequencing error, introgression, missing lineages, and gene-tree species-tree discordance.[89–92] Methodological advances on these fronts are required to enable more robust tests of macroevolutionary hypotheses linking dispersal traits, biogeography, and rates of speciation and extinction.

Conclusions

Using global-scale analyses based on a time tree of over 9,000 bird species, we found a strong positive relationship between dispersal ability and geographic range size, supporting a prominent role of flight efficiency in avian range expansion.[40] In contrast, we found a negative effect of speciation on geographic range size, revealing the footprint of recent speciation history on current geographical distributions. Speciation rates were slightly higher among dispersive lineages, which may be caused by speciation after dispersal or due to lower population sizes among dispersive lineages reducing levels of gene flow and enhancing their chances of speciation. We conclude that the macro-scale interplay between dispersal, geographic range size, and speciation is characterized by complex cause-effect asymmetries in which geographic range size is an outcome of dispersal and speciation, whereas variation in speciation rates may be driven by additional factors, including population size, climate, and geological history. This study opens new avenues of research into the origins and structure of global bird diversity and also provides an expanded and updated phylogenetic framework for addressing current and future challenges in macroecology and macroevolution.

RESOURCE AVAILABILITY

Lead contact

Requests for further information should be directed to the lead contact, Santiago Claramunt (sclaramu@uno.edu).

Materials availability

This study did not generate any new materials.

Data and code availability

- DNA sequence data are available in the Zenodo data repository at https://10.5281/zenodo.13377013. New DNA sequences generated in this study were deposited in GenBank.
- Code for reproducing results is available in the Zenodo data repository at https://10.5281/zenodo.13377013. Code for assembling the bird phylogeny and the resultant tree files can also be found at https://github.com/evolucionario/bigbirdtree
- Any additional information required to reanalyze the data reported in this paper is available from the lead contact upon request.

ACKNOWLEDGMENTS

We thank the many researchers who contributed data to the underlying datasets and the museum curators and collections managers who allowed access to specimens, particularly the Natural History Museum, Tring, and the

American Museum of Natural History. We thank Oliver Haddrath for sequencing new samples at the Royal Ontario Museum and Alexandra Margaritescu for assistance in locating sources of phylogenetic information. We are grateful to Gavin Thomas, Rich Grenyer, and Nathalie Seddon for helpful comments on a previous version of this manuscript. This study was funded by grants from the Natural Environment Research Council (NE/I028068/1 and NE/K016385/1; J.T.), the European Research Council (788203; C.S.), and the Natural Sciences and Engineering Research Council of Canada (RGPIN-2018-06747; S.C.).

AUTHOR CONTRIBUTIONS

S.C., C.S., B.C.W., and J.A.T. conceived the study. S.C. and J.C. produced the calibrated backbone tree. J.W.B. generated subclade trees from GenBank data. S.C. and M.M.S. assembled the comprehensive tree of birds. S.C., C. S., G.C.-R., J.A.T., and B.C.W. collected and compiled species trait data. S. C. wrote the manuscript with help from C.S., B.C.W., and J.A.T. All authors revised the manuscript.

DECLARATION OF INTERESTS

The authors declare no competing interests.

STAR★METHODS

Detailed methods are provided in the online version of this paper and include the following:

- KEY RESOURCES TABLE
- EXPERIMENTAL MODEL AND STUDY PARTICIPANT DETAILS
- METHOD DETAILS
- QUANTIFICATION AND STATISTICAL ANALYSIS
  - A new time-tree of the world's birds
  - Lineage-specific speciation rates
  - Dispersal proxies and geographic data
  - Phylogenetic Linear Models
  - Trait-dependent speciation and extinction

SUPPLEMENTAL INFORMATION

Supplemental information can be found online at https://doi.org/10.1016/j.cub.2025.07.004.

Received: September 13, 2024
Revised: May 19, 2025
Accepted: July 1, 2025

REFERENCES

1. Brown, J.H., and Maurer, B.A. (1987). Evolution of species assemblages: Effects of energetic constraints and species dynamics on the diversification of the North American avifauna. Am. Nat. *130*, 1–17. https://doi.org/10.1086/284694.
2. Rosenzweig, M.L. (1995). Species Diversity in Space and Time (Cambridge University Press). https://doi.org/10.1017/CBO9780511623387.
3. Birand, A., Vose, A., and Gavrilets, S. (2012). Patterns of species ranges, speciation, and extinction. Am. Nat. *179*, 1–21. https://doi.org/10.1086/663202.
4. Tobias, J.A., Ottenburghs, J., and Pigot, A.L. (2020). Avian diversity: Speciation, macroevolution, and ecological function. Annu. Rev. Ecol. Evol. Syst. *51*, 533–560. https://doi.org/10.1146/annurev-ecolsys-110218-025023.
5. Alzate, A., and Onstein, R.E. (2022). Understanding the relationship between dispersal and range size. Ecol. Lett. *25*, 2303–2323. https://doi.org/10.1111/ele.14089.
6. Bastidas-Urrutia, A.M., Biber, M.F., Böhning-Gaese, K., Fritz, S.A., Kreft, H., Tobias, J.A., Weigelt, P., and Hof, C. (2025). Species traits and island biogeography: Wing metrics linked to avian dispersal ability predict species occurrence on remote islands worldwide. J. Biogeogr. *52*, 350–361. https://doi.org/10.1111/jbi.15038.
7. Lester, S.E., Ruttenberg, B.I., Gaines, S.D., and Kinlan, B.P. (2007). The relationship between dispersal ability and geographic range size. Ecol. Lett. *10*, 745–758. https://doi.org/10.1111/j.1461-0248.2007.01070.x.
8. Gaston, K.J. (1998). Species-range size distributions: products of speciation, extinction and transformation. Phil. Trans. R. Soc. Lond. B *353*, 219–230. https://doi.org/10.1098/rstb.1998.0204.
9. Takashina, N., Plank, M.J., Jenkins, C.N., and Economo, E.P. (2022). Species-range-size distributions: Integrating the effects of speciation, transformation, and extinction. Ecol. Evol. *12*, e8341. https://doi.org/10.1002/ece3.8341.
10. Mayr, E. (1963). Animal Species and Evolution (Harvard University Press). https://doi.org/10.4159/harvard.9780674865327.
11. Coyne, J.A., and Orr, H.A. (2004). Speciation (Oxford University Press).
12. Price, T. (2008). Speciation in Birds (W. H. Freeman).
13. Claramunt, S., Derryberry, E.P., Remsen, J.V., Jr., and Brumfield, R.T. (2012). High dispersal ability inhibits speciation in a continental radiation of passerine birds. Proc. Biol. Sci. *279*, 1567–1574. https://doi.org/10.1098/rspb.2011.1922.
14. Mayr, E., and Diamond, J.M. (2001). The Birds of Northern Melanesia: Speciation, Ecology & Biogeography (Oxford University Press). https://doi.org/10.1093/oso/9780195141702.001.0001.
15. Yamaguchi, R. (2022). Intermediate dispersal hypothesis of species diversity: New insights. Ecol. Res. *37*, 301–315. https://doi.org/10.1111/1440-1703.12313.
16. Yamaguchi, R., and Iwasa, Y. (2013). First passage time to allopatric speciation. Interface Focus *3*, 20130026. https://doi.org/10.1098/rsfs.2013.0026.
17. Ciccheto, J.R.M., Carnaval, A.C., and Araujo, S.B.L. (2024). The influence of fragmented landscapes on speciation. J. Evol. Biol. *37*, 1499–1509. https://doi.org/10.1093/jeb/voae043.
18. Weeks, B.C., and Claramunt, S. (2014). Dispersal has inhibited avian diversification in Australasian archipelagoes. Proc. Biol. Sci. *281*, 20141257. https://doi.org/10.1098/rspb.2014.1257.
19. Hay, E.M., McGee, M.D., and Chown, S.L. (2022). Geographic range size and speciation in honeyeaters. BMC Ecol. Evol. *22*, 86. https://doi.org/10.1186/s12862-022-02041-6.
20. Tobias, J.A., Sheard, C., Pigot, A.L., Devenish, A.J.M., Yang, J., Sayol, F., Neate-Clegg, M.H.C., Alioravainen, N., Weeks, T.L., Barber, R.A., et al. (2022). AVONET: morphological, ecological and geographical data for all birds. Ecol. Lett. *25*, 581–597. https://doi.org/10.1111/ele.13898.
21. Hartfelder, J., Reynolds, C., Stanton, R.A., Sibiya, M., Monadjem, A., McCleery, R.A., and Fletcher, R.J. (2020). The allometry of movement predicts the connectivity of communities. Proc. Natl. Acad. Sci. USA *117*, 22274–22280. https://doi.org/10.1073/pnas.2001614117.
22. Jenkins, D.G., Brescacin, C.R., Duxbury, C.V., Elliott, J.A., Evans, J.A., Grablow, K.R., Hillegass, M., Lyon, B.N., Metzger, G.A., Olandese, M.L., et al. (2007). Does size matter for dispersal distance? Glob. Ecol. Biogeogr. *16*, 415–425. https://doi.org/10.1111/j.1466-8238.2007.00312.x.
23. Sutherland, G.D., Harestad, A.S., Price, K., and Lertzman, K. (2000). Scaling of natal dispersal distances in terrestrial birds and mammals. Conserv. Ecol. *4*, 16. https://doi.org/10.5751/ES-00184-040116.
24. Claramunt, S. (2021). Flight efficiency explains differences in natal dispersal distances in birds. Ecology *102*, e03442. https://doi.org/10.1002/ecy.3442.
25. Claramunt, S., and Wright, N.A. (2017). Using museum specimens to study flight and dispersal. In The Extended Specimen Studies in Avian Biology, M.S. Webster, ed. (CRC Press), pp. 127–141.
26. Weeks, B.C., O'Brien, B.K., Chu, J.J., Claramunt, S., Sheard, C., and Tobias, J.A. (2022). Morphological adaptations linked to flight efficiency

and aerial lifestyle determine natal dispersal distance in birds. Funct. Ecol. *36*, 1681–1689. https://doi.org/10.1111/1365-2435.14056.

27. Hernández, C.E., Rodríguez-Serrano, E., Avaria-Llautureo, J., Inostroza-Michael, O., Morales-Pallero, B., Boric-Bargetto, D., Canales-Aguirre, C. B., Marquet, P.A., and Meade, A. (2013). Using phylogenetic information and the comparative method to evaluate hypotheses in macroecology. Methods Ecol. Evol. *4*, 401–415. https://doi.org/10.1111/2041-210X.12033.
28. Morlon, H., Andréoletti, J., Barido-Sottani, J., Lambert, S., Perez-Lamarque, B., Quintero, I., Senderov, V., and Veron, P. (2024). Phylogenetic insights into diversification. Annu. Rev. Ecol. Evol. Syst. *55*, 1–21. https://doi.org/10.1146/annurev-ecolsys-102722-020508.
29. Burleigh, J.G., Kimball, R.T., and Braun, E.L. (2015). Building the avian tree of life using a large-scale, sparse supermatrix. Mol. Phylogenet. Evol. *84*, 53–63. https://doi.org/10.1016/j.ympev.2014.12.003.
30. Jetz, W., Thomas, G.H., Joy, J.B., Hartmann, K., and Mooers, A.O. (2012). The global diversity of birds in space and time. Nature *491*, 444–448. https://doi.org/10.1038/nature11631.
31. McTavish, E.J., Gerbracht, J.A., Holder, M.T., Iliff, M.J., Lepage, D., Rasmussen, P.C., Redelings, B.D., Sánchez Reyes, L.L., and Miller, E. T. (2025). A complete and dynamic tree of birds. Proc. Natl. Acad. Sci. USA *122*, e2409658122. https://doi.org/10.1073/pnas.2409658122.
32. Hackett, S.J., Kimball, R.T., Reddy, S., Bowie, R.C.K., Braun, E.L., Braun, M.J., Chojnowski, J.L., Cox, W.A., Han, K.-L., Harshman, J., et al. (2008). A phylogenomic study of birds reveals their evolutionary history. Science *320*, 1763–1768. https://doi.org/10.1126/science.1157704.
33. Claramunt, S., Braun, E.L., Cracraft, J., Fjeldså, J., Ho, S.Y.W., Houde, P., Nguyen, J.M.T., and Stiller, J. (2024). Calibrating the genomic clock of modern birds using fossils. Proc. Natl. Acad. Sci. USA *121*, e2405887121. https://doi.org/10.1073/pnas.2405887121.
34. Claramunt, S., and Cracraft, J. (2015). A new time tree reveals Earth history's imprint on the evolution of modern birds. Sci. Adv. *1*, e1501005. https://doi.org/10.1126/sciadv.1501005.
35. Stiller, J., Feng, S., Chowdhury, A.-A., Rivas-González, I., Duchêne, D.A., Fang, Q., Deng, Y., Kozlov, A., Stamatakis, A., Claramunt, S., et al. (2024). Complexity of avian evolution revealed by family-level genomes. Nature *629*, 851–860. https://doi.org/10.1038/s41586-024-07323-1.
36. Maliet, O., and Morlon, H. (2022). Fast and accurate estimation of species-specific diversification rates using data augmentation. Syst. Biol. *71*, 353–366. https://doi.org/10.1093/sysbio/syab055.
37. Braun, E.L., Cracraft, J., and Houde, P. (2019). Resolving the avian tree of life from top to bottom: the promise and potential boundaries of the phylogenomic era. In Avian Genomics in Ecology and Evolution: From the Lab into the Wild, R.H.S. Kraus, ed. (Springer International Publishing), pp. 151–210. https://doi.org/10.1007/978-3-030-16477-5_6.
38. Maliet, O., Hartig, F., and Morlon, H. (2019). A model with many small shifts for estimating species-specific diversification rates. Nat. Ecol. Evol. *3*, 1086–1092. https://doi.org/10.1038/s41559-019-0908-0.
39. Smyčka, J., Toszogyova, A., and Storch, D. (2023). The relationship between geographic range size and rates of species diversification. Nat. Commun. *14*, 5559. https://doi.org/10.1038/s41467-023-41225-6.
40. Sheard, C., Neate-Clegg, M.H.C., Alioravainen, N., Jones, S.E.I., Vincent, C., MacGregor, H.E.A., Bregman, T.P., Claramunt, S., and Tobias, J.A. (2020). Ecological drivers of global gradients in avian dispersal inferred from wing morphology. Nat. Commun. *11*, 2463. https://doi.org/10.1038/s41467-020-16313-6.
41. Baldwin, J.W., Garcia-Porta, J., and Botero, C.A. (2023). Complementarity in Allen's and Bergmann's rules among birds. Nat. Commun. *14*, 4240. https://doi.org/10.1038/s41467-023-39954-9.
42. Stevens, G.C. (1989). The latitudinal gradient in geographical range: how so many species coexist in the tropics. Am. Nat. *133*, 240–256. https://doi.org/10.1086/284913.
43. FitzJohn, R.G. (2010). Quantitative traits and diversification. Syst. Biol. *59*, 619–633. https://doi.org/10.1093/sysbio/syq053.
44. Beaulieu, J.M., and O'Meara, B.C. (2016). Detecting hidden diversification shifts in models of trait-dependent speciation and extinction. Syst. Biol. *65*, 583–601. https://doi.org/10.1093/sysbio/syw022.
45. Harvey, M.G., and Rabosky, D.L. (2018). Continuous traits and speciation rates: Alternatives to state-dependent diversification models. Methods Ecol. Evol. *9*, 984–993. https://doi.org/10.1111/2041-210X.12949.
46. Arango, A., Pinto-Ledezma, J., Rojas-Soto, O., Lindsay, A.M., Mendenhall, C.D., and Villalobos, F. (2022). Hand-Wing Index as a surrogate for dispersal ability: the case of the Emberizoidea (Aves: Passeriformes) radiation. Biol. J. Linn. Soc. *137*, 137–144. https://doi.org/10.1093/biolinnean/blac071.
47. Norberg, U.M. (1990). Vertebrate Flight (Springer Berlin Heidelberg). https://doi.org/10.1007/978-3-642-83848-4.
48. Pennycuick, C.J. (2008). Modelling the Flying Bird (Elsevier).
49. Taylor, G.K., and Thomas, A.L.R. (2014). Evolutionary Biomechanics: Selection, Phylogeny, and Constraint (Oxford University Press).
50. Chu, J.J., and Claramunt, S. (2023). Determinants of natal dispersal distances in North American birds. Ecol. Evol. *13*, e9789. https://doi.org/10.1002/ece3.9789.
51. Claramunt, S., Hong, M., and Bravo, A. (2022). The effect of flight efficiency on gap-crossing ability in Amazonian forest birds. Biotropica *54*, 860–868. https://doi.org/10.1111/btp.13109.
52. Naka, L.N., Costa, B.M. da S., Lima, G.R., and Claramunt, S. (2022). Riverine barriers as obstacles to dispersal in amazonian birds. Front. Ecol. Evol. *10*, 846975. https://doi.org/10.3389/fevo.2022.846975.
53. Gaston, K., and Blackburn, T. (2000). Pattern and Process in Macroecology (John Wiley & Sons).
54. Clauset, A., and Erwin, D.H. (2008). The evolution and distribution of species body size. Science *321*, 399–401. https://doi.org/10.1126/science.1157534.
55. Inostroza-Michael, O., Hernández, C.E., Rodríguez-Serrano, E., Avaria-Llautureo, J., and Rivadeneira, M.M. (2018). Interspecific geographic range size–body size relationship and the diversification dynamics of Neotropical furnariid birds. Evolution *72*, 1124–1133. https://doi.org/10.1111/evo.13481.
56. Cadena, C.D., Cuervo, A.M., Céspedes, L.N., Bravo, G.A., Krabbe, N., Schulenberg, T.S., Derryberry, G.E., Silveira, L.F., Derryberry, E.P., Brumfield, R.T., et al. (2020). Systematics, biogeography, and diversification of Scytalopus tapaculos (Rhinocryptidae), an enigmatic radiation of Neotropical montane birds. Auk *137*, 1–30. https://doi.org/10.1093/auk/ukz077.
57. Phillimore, A.B., Freckleton, R.P., Orme, C.D.L., and Owens, I.P.F. (2006). Ecology predicts large-scale patterns of phylogenetic diversification in birds. Am. Nat. *168*, 220–229. https://doi.org/10.1086/505763.
58. Jønsson, K.A., Fabre, P.-H., Ricklefs, R.E., and Fjeldså, J. (2011). Major global radiation of corvoid birds originated in the proto-Papuan archipelago. Proc. Natl. Acad. Sci. USA *108*, 2328–2333. https://doi.org/10.1073/pnas.1018956108.
59. McCullough, J.M., Oliveros, C.H., Benz, B.W., Zenil-Ferguson, R., Cracraft, J., Moyle, R.G., and Andersen, M.J. (2022). Wallacean and Melanesian islands promote higher rates of diversification within the global passerine radiation Corvides. Syst. Biol. *71*, 1423–1439. https://doi.org/10.1093/sysbio/syac044.
60. Arango, A., Pinto-Ledezma, J., Rojas-Soto, O., and Villalobos, F. (2025). Broad geographic dispersal is not a diversification driver for Emberizoidea. Proc. Biol. Sci. *292*, 20241965. https://doi.org/10.1098/rspb.2024.1965.
61. Imfeld, T.S., and Barker, F.K. (2022). Songbirds of the Americas show uniform morphological evolution despite heterogeneous diversification. J. Evol. Biol. *35*, 1335–1351. https://doi.org/10.1111/jeb.14084.
62. Imfeld, T.S., and Barker, F.K. (2024). Passerine sister clade comparisons reveal variable macroevolutionary outcomes of interhemispheric dispersal. J. Evol. Biol. *37*, 37–50. https://doi.org/10.1093/jeb/voad001.

63. Wright, N.A., Steadman, D.W., and Witt, C.C. (2016). Predictable evolution toward flightlessness in volant island birds. Proc. Natl. Acad. Sci. USA *113*, 4765–4770. https://doi.org/10.1073/pnas.1522931113.

64. Valente, L., Phillimore, A.B., Melo, M., Warren, B.H., Clegg, S.M., Havenstein, K., Tiedemann, R., Illera, J.C., Thébaud, C., Aschenbach, T., et al. (2020). A simple dynamic model explains the diversity of island birds worldwide. Nature *579*, 92–96. https://doi.org/10.1038/s41586-020-2022-5.

65. Dufour, P., Sayol, F., Cooke, R., Blackburn, T.M., Gallien, L., Griesser, M., Steinbauer, M.J., and Faurby, S. (2024). The importance of migratory drop-off for island colonization in birds. Proc. Biol. Sci. *291*, 20232926. https://doi.org/10.1098/rspb.2023.2926.

66. Gómez-Bahamón, V., Márquez, R., Jahn, A.E., Miyaki, C.Y., Tuero, D.T., Laverde-R, O., Restrepo, S., and Cadena, C.D. (2020). Speciation associated with shifts in migratory behavior in an avian radiation. Curr. Biol. *30*, 1312–1321.e6. https://doi.org/10.1016/j.cub.2020.01.064.

67. Paradis, E., Baillie, S.R., Sutherland, W.J., and Gregory, R.D. (1998). Patterns of natal and breeding dispersal in birds. J. Anim. Ecol. *67*, 518–536. https://doi.org/10.1046/j.1365-2656.1998.00215.x.

68. Santini, L., Tobias, J.A., Callaghan, C., Gallego-Zamorano, J., and Benítez-López, A. (2023). Global patterns and predictors of avian population density. Glob. Ecol. Biogeogr. *32*, 1189–1204. https://doi.org/10.1111/geb.13688.

69. Slatkin, M. (1987). Gene flow and the geographic structure of natural populations. Science *236*, 787–792. https://doi.org/10.1126/science.3576198.

70. Wright, S. (1931). Evolution in mendelian populations. Genetics *16*, 97–159. https://doi.org/10.1093/genetics/16.2.97.

71. Freeman, B.G., Montgomery, G.A., Heavyside, J., Moncrieff, A.E., Johnson, O., and Winger, B.M. (2023). On the predictability of phenotypic divergence in geographic isolation. Evolution *77*, 26–35. https://doi.org/10.1093/evolut/qpac040.

72. Harvey, M.G., Seeholzer, G.F., Smith, B.T., Rabosky, D.L., Cuervo, A.M., and Brumfield, R.T. (2017). Positive association between population genetic differentiation and speciation rates in New World birds. Proc. Natl. Acad. Sci. USA *114*, 6328–6333. https://doi.org/10.1073/pnas.1617397114.

73. Smith, B.T., Seeholzer, G.F., Harvey, M.G., Cuervo, A.M., and Brumfield, R.T. (2017). A latitudinal phylogeographic diversity gradient in birds. PLoS Biol. *15*, e2001073. https://doi.org/10.1371/journal.pbio.2001073.

74. Kittelberger, K.D., Tanner, C.J., Buxton, A.N., Prewett, A., and Şekercioğlu, Ç.H. (2024). Correlates of avian extinction timing around the world since 1500 CE. Avian Res. *15*, 100213. https://doi.org/10.1016/j.avrs.2024.100213.

75. Matthews, T.J., Triantis, K.A., Wayman, J.P., Martin, T.E., Hume, J.P., Cardoso, P., Faurby, S., Mendenhall, C.D., Dufour, P., Rigal, F., et al. (2024). The global loss of avian functional and phylogenetic diversity from anthropogenic extinctions. Science *386*, 55–60. https://doi.org/10.1126/science.adk7898.

76. Cooke, R., Sayol, F., Andermann, T., Blackburn, T.M., Steinbauer, M.J., Antonelli, A., and Faurby, S. (2023). Undiscovered bird extinctions obscure the true magnitude of human-driven extinction waves. Nat. Commun. *14*, 8116. https://doi.org/10.1038/s41467-023-43445-2.

77. Pulido-Santacruz, P., and Weir, J.T. (2016). Extinction as a driver of avian latitudinal diversity gradients. Evolution *70*, 860–872. https://doi.org/10.1111/evo.12899.

78. Pyron, R.A., and Wiens, J.J. (2013). Large-scale phylogenetic analyses reveal the causes of high tropical amphibian diversity. Proc. Biol. Sci. *280*, 20131622. https://doi.org/10.1098/rspb.2013.1622.

79. Quintero, I., Landis, M.J., Jetz, W., and Morlon, H. (2023). The build-up of the present-day tropical diversity of tetrapods. Proc. Natl. Acad. Sci. USA *120*, e2220672120. https://doi.org/10.1073/pnas.2220672120.

80. Haffer, J. (1969). Speciation in Amazonian forest birds. Science *165*, 131–137. https://doi.org/10.1126/science.165.3889.131.

81. Musher, L.J., Giakoumis, M., Albert, J., Del-Rio, G., Rego, M., Thom, G., Aleixo, A., Ribas, C.C., Brumfield, R.T., Smith, B.T., et al. (2022). River network rearrangements promote speciation in lowland Amazonian birds. Sci. Adv. *8*, eabn1099. https://doi.org/10.1126/sciadv.abn1099.

82. Vrba, E.S. (1993). Turnover-pulses, the Red Queen, and related topics. Am. J. Sci. *293*, 418–452. https://doi.org/10.2475/ajs.293.A.418.

83. Elizangela dos Santos Barbosa, W.E. dos S., Ferreira, M., de Deus Schultz, E., Willians Luna, L., Orsi Laranjeiras, T., Aleixo, A., and Cherem Ribas, C. (2022). Habitat association constrains population history in two sympatric ovenbirds along Amazonian floodplains. J. Biogeogr. *49*, 1683–1695. https://doi.org/10.1111/jbi.14266.

84. Harvey, M.G., Aleixo, A., Ribas, C.C., and Brumfield, R.T. (2017). Habitat association predicts genetic diversity and population divergence in Amazonian birds. Am. Nat. *190*, 631–648. https://doi.org/10.1086/693856.

85. Johnson, O., Ribas, C.C., Aleixo, A., Naka, L.N., Harvey, M.G., and Brumfield, R.T. (2023). Amazonian birds in more dynamic habitats have less population genetic structure and higher gene flow. Mol. Ecol. *32*, 2186–2205. https://doi.org/10.1111/mec.16886.

86. Ribas, C.C., Aleixo, A., Nogueira, A.C.R., Miyaki, C.Y., and Cracraft, J. (2011). A palaeobiogeographic model for biotic diversification within Amazonia over the past three million years. Proc. R. Soc. B. *279*, 681–689. https://doi.org/10.1098/rspb.2011.1120.

87. Greenberg, D.A., and Mooers, A.Ø. (2017). Linking speciation to extinction: Diversification raises contemporary extinction risk in amphibians. Evol. Lett. *1*, 40–48. https://doi.org/10.1002/evl3.4.

88. Stanley, S.M. (1990). The general correlation between rate of speciation and rate of extinction: fortuitous causal linkages. In Causes of Evolution: A Paleontological Perspective, R.M. Ross, and W.D. Allmon, eds. (University of Chicago Press), pp. 103–127.

89. de Maio, N., Schrempf, D., and Kosiol, C. (2015). PoMo: An allele frequency-based approach for species tree estimation. Syst. Biol. *64*, 1018–1031. https://doi.org/10.1093/sysbio/syv048.

90. Faurby, S., Eiserhardt, W.L., and Svenning, J.-C. (2016). Strong effects of variation in taxonomic opinion on diversification analyses. Methods Ecol. Evol. *7*, 4–13. https://doi.org/10.1111/2041-210X.12449.

91. Harvey, M.G., Bravo, G.A., Claramunt, S., Cuervo, A.M., Derryberry, G. E., Battilana, J., Seeholzer, G.F., McKay, J.S., O'Meara, B.C., Faircloth, B.C., et al. (2020). The evolution of a tropical biodiversity hotspot. Science *370*, 1343–1348. https://doi.org/10.1126/science.aaz6970.

92. Tabatabaee, Y., Zhang, C., Warnow, T., and Mirarab, S. (2023). Phylogenomic branch length estimation using quartets. Bioinformatics *39*, i185–i193. https://doi.org/10.1093/bioinformatics/btad221.

93. Sayol, F., Steinbauer, M.J., Blackburn, T.M., Antonelli, A., and Faurby, S. (2020). Anthropogenic extinctions conceal widespread evolution of flightlessness in birds. Sci. Adv. *6*, eabb6095. https://doi.org/10.1126/sciadv.abb6095.

94. Maddison, W.P., and Maddison, D.R. (2018). Mesquite: a modular system for evolutionary analysis. Version 3.4. http://mesquiteproject.org.

95. Minh, B.Q., Schmidt, H.A., Chernomor, O., Schrempf, D., Woodhams, M.D., von Haeseler, A., and Lanfear, R. (2020). IQ-TREE 2: new models and efficient methods for phylogenetic inference in the genomic era. Mol. Biol. Evol. *37*, 1530–1534. https://doi.org/10.1093/molbev/msaa015.

96. Claramunt, S. (2022). CladeDate: Calibration information generator for divergence time estimation. Methods Ecol. Evol. *13*, 2331–2338. https://doi.org/10.1111/2041-210X.13977.

97. R Core Team (2023). R: The R Project for Statistical Computing (R Foundation for Statistical Computing). https://www.R-project.org/.

98. Paradis, E., and Schliep, K. (2019). ape 5.0: An environment for modern phylogenetics and evolutionary analyses in R. Bioinformatics *35*, 526–528. https://doi.org/10.1093/bioinformatics/bty633.

99. Smith, S.A., and Walker, J.F. (2019). PyPHLAWD: A python tool for phylogenetic dataset construction. Methods Ecol. Evol. *10*, 104–108. https://doi.org/10.1111/2041-210X.13096.

100. Bezanson, J., Karpinski, S., Shah, V.B., and Edelman, A. (2012). Julia: a fast dynamic language for technical computing. Preprint at arXiv. https://doi.org/10.48550/arXiv.1209.5145.

101. Hijmans, R.J., Etten, J. van, Sumner, M., Cheng, J., Baston, D., Bevan, A., Bivand, R., Busetto, L., Canty, M., Fasoli, B., et al. (2025). raster: geographic data analysis and modeling. Version 3.6-31.

102. Ho, T., and Ané, C. (2014). A linear-time algorithm for Gaussian and non-Gaussian trait evolution models. Syst. Biol. *63*, 397–408. https://doi.org/10.1093/sysbio/syu005.

103. van der Bijl, W. (2018). phylopath: Easy phylogenetic path analysis in R. PeerJ *6*, e4718. https://doi.org/10.7717/peerj.4718.

104. FitzJohn, R.G. (2012). Diversitree: comparative phylogenetic analyses of diversification in R. Methods Ecol. Evol. *3*, 1084–1092. https://doi.org/10.1111/j.2041-210X.2012.00234.x.

105. Louca, S., and Pennell, M.W. (2020). A general and efficient algorithm for the likelihood of diversification and discrete-trait evolutionary models. Syst. Biol. *69*, 545–556. https://doi.org/10.1093/sysbio/syz055.

106. Herrera-Alsina, L., van Els, P., and Etienne, R.S. (2019). Detecting the dependence of diversification on multiple traits from phylogenetic trees and trait data. Syst. Biol. *68*, 317–328. https://doi.org/10.1093/sysbio/syy057.

107. Almeida, F.C., Porzecanski, A.L., Cracraft, J.L., and Bertelli, S. (2022). The evolution of tinamous (Palaeognathae: Tinamidae) in light of molecular and combined analyses. Zool. J. Linn. Soc. *195*, 106–124. https://doi.org/10.1093/zoolinnean/zlab080.

108. Kimball, R.T., Hosner, P.A., and Braun, E.L. (2021). A phylogenomic supermatrix of Galliformes (Landfowl) reveals biased branch lengths. Mol. Phylogenet. Evol. *158*, 107091. https://doi.org/10.1016/j.ympev.2021.107091.

109. Černý, D., and Natale, R. (2022). Comprehensive taxon sampling and vetted fossils help clarify the time tree of shorebirds (Aves, Charadriiformes). Mol. Phylogenet. Evol. *177*, 107620. https://doi.org/10.1016/j.ympev.2022.107620.

110. McCullough, J.M., Moyle, R.G., Smith, B.T., and Andersen, M.J. (2019). A Laurasian origin for a pantropical bird radiation is supported by genomic and fossil data (Aves: Coraciiformes). Proc. Biol. Sci. *286*, 20190122. https://doi.org/10.1098/rspb.2019.0122.

111. Shakya, S.B., Fuchs, J., Pons, J.-M., and Sheldon, F.H. (2017). Tapping the woodpecker tree for evolutionary insight. Mol. Phylogenet. Evol. *116*, 182–191. https://doi.org/10.1016/j.ympev.2017.09.005.

112. Smith, B.T., Merwin, J., Provost, K.L., Thom, G., Brumfield, R.T., Ferreira, M., Mauck, W.M., III, Moyle, R.G., Wright, T.F., and Joseph, L. (2023). Phylogenomic analysis of the parrots of the world distinguishes artifactual from biological sources of gene tree discordance. Syst. Biol. *72*, 228–241. https://doi.org/10.1093/sysbio/syac055.

113. Marki, P.Z., Jønsson, K.A., Irestedt, M., Nguyen, J.M.T., Rahbek, C., and Fjeldså, J. (2017). Supermatrix phylogeny and biogeography of the Australasian Meliphagides radiation (Aves: Passeriformes). Mol. Phylogenet. Evol. *107*, 516–529. https://doi.org/10.1016/j.ympev.2016.12.021.

114. Cai, T., Cibois, A., Alström, P., Moyle, R.G., Kennedy, J.D., Shao, S., Zhang, R., Irestedt, M., Ericson, P.G.P., Gelang, M., et al. (2019). Near-complete phylogeny and taxonomic revision of the world's babblers (Aves: Passeriformes). Mol. Phylogenet. Evol. *130*, 346–356. https://doi.org/10.1016/j.ympev.2018.10.010.

115. Alström, P., Mohammadi, Z., Enbody, E.D., Irestedt, M., Engelbrecht, D., Crochet, P.-A., Guillaumet, A., Rancilhac, L., Tieleman, B.I., Olsson, U., et al. (2023). Systematics of the avian family Alaudidae using multilocus and genomic data. Avian Res. *14*, 100095. https://doi.org/10.1016/j.avrs.2023.100095.

116. Shakya, S.B., and Sheldon, F.H. (2017). The phylogeny of the world's bulbuls (Pycnonotidae) inferred using a supermatrix approach. Ibis *159*, 498–509. https://doi.org/10.1111/ibi.12464.

117. De Silva, T.N., Peterson, A.T., and Perktas, U. (2019). An extensive molecular phylogeny of weaverbirds (Aves: Ploceidae) unveils broad non-monophyly of traditional genera and new relationships. Auk *136*, ukz041. https://doi.org/10.1093/auk/ukz041.

118. Olsson, U., and Alström, P. (2020). A comprehensive phylogeny and taxonomic evaluation of the waxbills (Aves: Estrildidae). Mol. Phylogenet. Evol. *146*, 106757. https://doi.org/10.1016/j.ympev.2020.106757.

119. Barker, F.K., Burns, K.J., Klicka, J., Lanyon, S.M., and Lovette, I.J. (2015). New insights into New World biogeography: An integrated view from the phylogeny of blackbirds, cardinals, sparrows, tanagers, warblers, and allies. Auk *132*, 333–348. https://doi.org/10.1642/AUK-14-110.1.

120. Dunning, J.B. (2007). CRC Handbook of Avian Body Masses, Second Edition (CRC Press). https://doi.org/10.1201/9781420064452.

121. Tobias, J.A., and Pigot, A.L. (2019). Integrating behaviour and ecology into global biodiversity conservation strategies. Philos. Trans. R. Soc. Lond. B Biol. Sci. *374*, 20190012. https://doi.org/10.1098/rstb.2019.0012.

122. Baker, A.J., Pereira, S.L., and Paton, T.A. (2007). Phylogenetic relationships and divergence times of Charadriiformes genera: multigene evidence for the Cretaceous origin of at least 14 clades of shorebirds. Biol. Lett. *3*, 205–209. https://doi.org/10.1098/rsbl.2006.0606.

123. Barker, F.K., Barrowclough, G.F., and Groth, J.G. (2002). A phylogenetic hypothesis for passerine birds: taxonomic and biogeographic implications of an analysis of nuclear DNA sequence data. Proc. Biol. Sci. *269*, 295–308. https://doi.org/10.1098/rspb.2001.1883.

124. Groth, J.G., and Barrowclough, G.F. (1999). Basal divergences in birds and the phylogenetic utility of the nuclear RAG-1 gene. Mol. Phylogenet. Evol. *12*, 115–123. https://doi.org/10.1006/mpev.1998.0603.

125. Chernomor, O., von Haeseler, A., and Minh, B.Q. (2016). Terrace aware data structure for phylogenomic inference from supermatrices. Syst. Biol. *65*, 997–1008. https://doi.org/10.1093/sysbio/syw037.

126. Jarvis, E.D., Mirarab, S., Aberer, A.J., Li, B., Houde, P., Li, C., Ho, S.Y.W., Faircloth, B.C., Nabholz, B., Howard, J.T., et al. (2014). Whole-genome analyses resolve early branches in the tree of life of modern birds. Science *346*, 1320–1331. https://doi.org/10.1126/science.1253451.

127. Reddy, S., Kimball, R.T., Pandey, A., Hosner, P.A., Braun, M.J., Hackett, S.J., Han, K.-L., Harshman, J., Huddleston, C.J., Kingston, S., et al. (2017). Why do phylogenomic data dets yield conflicting trees? Data type influences the avian tree of life more than taxon sampling. Syst. Biol. *66*, 857–879. https://doi.org/10.1093/sysbio/syx041.

128. Marshall, C.R. (2019). Using the fossil record to evaluate timetree timescales. Front. Genet. *10*, 1049. https://doi.org/10.3389/fgene.2019.01049.

129. Parham, J.F., Donoghue, P.C.J., Bell, C.J., Calway, T.D., Head, J.J., Holroyd, P.A., Inoue, J.G., Irmis, R.B., Joyce, W.G., Ksepka, D.T., et al. (2012). Best practices for justifying fossil calibrations. Syst. Biol. *61*, 346–359. https://doi.org/10.1093/sysbio/syr107.

130. Clements, J.F., Schulenberg, T.S., Rasmussen, P.C., Iliff, M.J., Fredericks, T.A., Gerbracht, J.A., Lepage, D., Billerman, S.M., Sullivan, B.L., Wood, C.L. et al. (2022). The eBird/Clements checklist of Birds of the World: v2022. https://www.birds.cornell.edu/clementschecklist/download/.

131. UICN (2001). IUCN Red List Categories and Criteria. Version 3.1 (International Union for Conservation of Nature).

132. Coyne, J.A., and Price, T.D. (2000). Little evidence for sympatric speciation in island birds. Evolution *54*, 2166–2171. https://doi.org/10.1111/j.0014-3820.2000.tb01260.x.

133. K.P. Burnham, and D.R. Anderson, eds. (2004). Model Selection and Multimodel Inference (Springer New York). https://doi.org/10.1007/b97636.

134. Akaike, H. (1974). A new look at the statistical model identification. IEEE Trans. Automat. Contr. *19*, 716–723. https://doi.org/10.1109/TAC.1974.1100705.

135. von Hardenberg, A., and Gonzalez-Voyer, A. (2013). Disentangling evolutionary cause-effect relationships with phylogenetic confirmatory path analysis. Evolution *67*, 378–387. https://doi.org/10.1111/j.1558-5646.2012.01790.x.

136. Pagel, M. (1999). Inferring the historical patterns of biological evolution. Nature *401*, 877–884. https://doi.org/10.1038/44766.

137. Freckleton, R.P., Harvey, P.H., and Pagel, M. (2002). Phylogenetic analysis and comparative data: A test and review of evidence. Am. Nat. *160*, 712–726. https://doi.org/10.1086/343873.

138. Cardon, M., Loot, G., Grenouillet, G., and Blanchet, S. (2011). Host characteristics and environmental factors differentially drive the burden and pathogenicity of an ectoparasite: A multilevel causal analysis. J. Anim. Ecol. *80*, 657–667. https://doi.org/10.1111/j.1365-2656.2011.01804.x.

139. Shipley, B. (2013). The AIC model selection method applied to path analytic models compared using a d-separation test. Ecology *94*, 560–564. https://doi.org/10.1890/12-0976.1.

Please cite this article in press as: Claramunt et al., A new time tree of birds reveals the interplay between dispersal, geographic range size, and diversification, Current Biology (2025), https://doi.org/10.1016/j.cub.2025.07.004

STAR★METHODS

KEY RESOURCES TABLE

REAGENT or RESOURCE	SOURCE	IDENTIFIER
Biological samples		
Tissue samples of 23 bird specimens.	American Museum of Natural History, New York, and Royal Ontario Museum, Toronto.	See file "Neornithes RAG Genes Dataset.nex" Zenodo: https://10.5281/zenodo.13377013
Critical commercial assays		
DNeasy Blood & Tissue Kit	Quiagen	69504
Deposited data		
Alignment RAG1 and RAG2 genes	This paper	"Neornithes RAG Genes Dataset.nex" Zenodo: https://10.5281/zenodo.13377013 GitHub: https://github.com/evolucionario/bigbirdtree
Maximum likelihood backbone and subclade phylogenies	This paper	Various ".tre" files. Zenodo: https://10.5281/zenodo.13377013 GitHub: https://github.com/evolucionario/bigbirdtree
List of fossils used for time calibration	This paper	CalibrationFossilsRAGtreeTEMPO.xls, Zenodo: https://10.5281/zenodo.13377013 GitHub: https://github.com/evolucionario/bigbirdtree
Calibrated backbone phylogeny	This paper	ChronogramNeornithes.nex, Zenodo: https://10.5281/zenodo.13377013 GitHub: https://github.com/evolucionario/bigbirdtree
Assembled composite tree of birds	This paper	BBtree.tre, BBtree2.tre, BBtree3.tre, BBtree C2022.tre. GitHub: https://10.5281/zenodo.1337701
Morphological and geographic data for all birds	Tobias et al.[20]	AVONET1_BirdLife.csv
Morphological and geographic data for all birds	Sheard et al.[40]	Dataset HWI 2020-04-10.xlsx
Classification of island birds	Sayol et al.[93]	DataFileS1and2Sayol.xlsx
Software and algorithms		
Mesquite 3.4	Maddison and Maddison[94]	https://www.mesquiteproject.org
IQ-TREE	Minh et al.[95]	http://www.iqtree.org
CladeDate 1.2	Claramunt[96]	https://github.com/evolucionario/CladeDate
R	R Core Team[97]	https://www.R-project.org/
ape 5.6	Paradis and Schliep[98]	https://github.com/emmanuelparadis/ape
Code for performing time-tree calibration in R	This paper	Chronos RAG calibration FINAL.R. Zenodo: https://10.5281/zenodo.13377013 GitHub: https://github.com/evolucionario/bigbirdtree
PyPHLAWD	Smith and Walker[99]	https://fephyfofum.github.io/PyPHLAWD/
Julia 1.9	Bezanson et al.[100]	https://julialang.org
raster v3.6	Hijmans et al.[101]	https://rspatial.org/raster/
PANDA	Maliet and Morlon[36]	https://hmorlon.github.io/PANDA.jl/dev/
phylolm 2.6.2.	Ho and Ané[102]	https://github.com/lamho86/phylolm
phylopath 1.1.3	Van der Bijl[103]	https://ax3man.github.io/phylopath/
diversitree 0.10-1	Fitzjohn[104]	https://www.zoology.ubc.ca/prog/diversitree/
castor 1.8.3	Louca and Pennell[105]	https://cran.r-project.org/web/packages/castor/index.html
secsse 3.1.0	Herrera-Alsina et al.[106]	https://cran.r-project.org/web/packages/secsse/index.html

Please cite this article in press as: Claramunt et al., A new time tree of birds reveals the interplay between dispersal, geographic range size, and diversification, Current Biology (2025), https://doi.org/10.1016/j.cub.2025.07.004

EXPERIMENTAL MODEL AND STUDY PARTICIPANT DETAILS

To generate a backbone tree of avian families, we compiled an alignment of sequences of Recombination Activation Genes (RAG) 1 and 2. We started with the alignment from Claramunt & Cracraft,[34] adding 2 crocodilians as outgroup and an additional 23 samples to complete the family-level coverage. The additional samples were obtained from GenBank or sequenced at the American Museum of Natural History and the Royal Ontario Museum from frozen tissue collections.

Phylogenies of subclades were obtained from previous studies or newly inferred from sequences deposited in GenBank as follow. We used high-quality phylogenetic trees of bird groups that were as complete as possible, including those of the Tinamidae,[107] Galliformes,[108] Charadriiformes,[109] Coraciiformes,[110] Picidae,[111] Psittaciformes,[112] Tyranni,[91] Melliphagidae,[113] Corvides,[59] Sylvioidea,[114] Alaudidae,[115] Pycnonotidae,[116] Ploceidae,[117] Estrildidae,[118] and Emberizoidea.[119] See the Zenodo data supplement for a full list source references for phylogenetic information (Zenodo: https://10.5281/zenodo.13377013).

We obtained data on average Hand-wing index, body mass, centroid latitude, and geographic range size from the AVONET database.[20] Body mass was originally based on Dunning,[120] with updates from primary and secondary literature.[121] Geographic range size was calculated for breeding and resident ranges of extant, native or reintroduced species, based on 2018 maps published by BirdLife International. Island dwelling was based on the classification of island endemic birds from Sayol et al.[93] We also conducted alterative analysis using the percentage of species distribution that occurs on islands, obtained from Sheard et al.[40]

METHOD DETAILS

For additional samples, DNA was extracted from frozen collections using DNeasy Blood and Tissue kits (Qiagen). Target sequences were amplified via PCR using previous protocols and primers for RAG1 and RAG2 sequencing.[122–124] PCR products were cleaned and cycle sequenced with dye terminator chemistry and run in Applied Biosystems genetic analyzers. The alignment of 324 terminals and 4,068 sites was assembled in Mesquite 3.4[94] and is provided in the data supplement, along with information on museum vouchers and GenBank accession numbers (Zenodo: https://10.5281/zenodo.13377013). The average percentage of missing, gap or ambiguous sites was 5%, and only 8 species were more than 50% incomplete, lacking sequences of the longer RAG1 gene.

QUANTIFICATION AND STATISTICAL ANALYSIS

A new time-tree of the world's birds

We generated a large-scale time-tree of modern birds using a sequential approach. We first estimated a time-calibrated backbone tree including at least one representative of all extant bird families using the alignment of RAG1 and RAG2 sequences. We inferred a maximum likelihood phylogram in *IQ-TREE*[95] using automatic identification of an optimal partitioning scheme (by gene and codon position) and nucleotide substitution model (*ModelFinder* algorithm[125]). We provided a reference partial topology to enforce the monophyly of calibration clades and other clades that are strongly supported by recent phylogenomic analyses.[32,126,127]

We derived time-calibration information empirically from the fossil record using estimators of the lower bounds of truncated distributions.[128] We selected 33 calibration nodes distributed across all major subclades of birds, based on strong evidence of clade monophyly and the existence of high-quality old fossils.[129] We then recorded the first fossil occurrence of each calibration clade on each continent in order to obtain a sample of the first occurrences for each clade.[34] Using the *CladeDate* package[96] in R,[97] we generated point estimates and confidence intervals for the age of the calibration nodes based on the fossil record of each clade. We transformed the phylogram into a time-calibrated ultrametric tree with the function *chronos* in the R package *ape* 5.6[98] using a mixture model of discrete rate categories as a relaxed molecular clock and estimates of the ages of 33 clades as calibration points.

Finally, we augmented the backbone tree by adding species-level phylogenies obtained from previous studies or newly inferred from GenBank sequence data. For the latter, we constructed multilocus alignments using PyPHLAWD in Python,[99] and inferred maximum likelihood trees with *IQ-TREE*. To time-calibrate these subtrees, we used *chronos* with a fixed age constraint on a node shared with the calibrated backbone. For subtrees based on calibrated Bayesian time-trees, we rescaled branch lengths to match the age of a corresponding node in our backbone. We then grafted the resulting subtrees into the backbone tree.

Lineage-specific speciation rates

We estimated lineage-specific speciation rates using the Bayesian ClaDS2 algorithm.[38] ClaDS2 assumes that each branch of the tree has its own speciation rate, and that the turnover (extinction/speciation) is constant. We used the Julia 1.9[100] implementation of ClaDS2 in the *PANDA* package, which relies on data augmentation to account for unsampled species.[36] We calculated family-level sampling fractions by dividing the number of species included in the tree by the total number of species in the eBird/Clements taxonomy.[130]

We then projected speciation rates on a world map using the *raster* v3.6 R package[101] at the 1°x1° scale using the 2019.1 BirdLife International range maps for resident and breeding populations. To avoid visual distortions, under-sampled grid cells with fewer than 15 species were omitted.

Please cite this article in press as: Claramunt et al., A new time tree of birds reveals the interplay between dispersal, geographic range size, and diversification, Current Biology (2025), https://doi.org/10.1016/j.cub.2025.07.004

Dispersal proxies and geographic data

To assess the dispersal propensity of species we used two proxies: body mass and Hand-wing index (HWI). HWI is a proxy for wing aspect ratio expressing the relationship between the length and the width of the hand portion of the wing. The wing length (*WL*) is the distance from the carpal joint to the tip of longest primary wing feather. Wing width (*S1*) can be measured either directly as the distance from the carpal joint to the tip of the first (most distal) secondary feather or indirectly (relative to *WL*) by measuring Kipp's distance, the distance from the tip of the longest primary feather to the tip of the first secondary (K_d). In the latter case the Hand-wing index is $100*K_d/WL$. Body mass is a single estimate, averaged where possible between males and females. Island dwelling from Sayol et al.[93] was included in analyses as a discrete binary variable. We also conducted alternative analyses using a low threshold island size of 2,000 km^2 to capture changes in eco-evolutionary dynamics associated with small islands, including increased extinction risk[131] and absence of intra-island speciation.[132] For this alternative analysis, the percentage of species distribution that occurs on islands was obtained from Sheard et al.[40] and treated as a continuous variable.

Phylogenetic Linear Models

We evaluated models of trait evolution and the strength of phylogenetic inertia for continuous dispersal traits and geographic factors using intercept-only models in the R package *phylolm* 2.6.2.[102] We compared models using the Akaike Information Criterion (AIC) and model selection techniques (Table S1).[133,134] We log-transformed body mass, geographic range size, and speciation rates to better conform with model assumptions of homoscedasticity and lack of bounds (e.g. rates bounded at zero). The absolute value of latitude was used to reflect change from tropical to polar regardless of hemisphere.

We then evaluated causal models of the relationships between factors using phylogenetic path analysis[135] with the R package *phylopath* v.1.1.3.[103] Phylogenetic non-independence of model residuals was modelled using a lambda-transformation of branch lengths[136] controlling for levels of phylogenetic inertia, with lambda estimated together with other model parameters.[137] We evaluated two models; in both, the two dispersal proxies (body mass and the Hand-wing index) affect speciation rate and geographic range size. In one model, the speciation rate affects geographic range size, whereas in the alternative model geographic range size affects the speciation rate. In both models, these four factors are affected by the two geographical covariates—latitude and island dwelling. As before, body mass, geographic range size, and speciation rates were log-transformed.

We did not model an effect of body mass on the Hand-wing index because body size is not expected to be related to a size-free shape variable such as the Hand-wing index; both small and large birds can have either very low or very high aspect ratio wings and the slope of a regression of log-body mass on HWI was not statistically different from zero (coefficient = -0.061, t = -0.21, P = 0.83). *Phylopath* uses the *phylolm* function to model causal effects, for which we used a 'lambda' correlation structure. The goodness of fit of alternative models was evaluated using the *d*-separation test based on Fisher's *C* statistic and a Chi-square distribution with 2 degrees of freedom.[135] We then compared models and estimated model-averaged parameters using a modified version of the Akaike Information Criterion based on the *C* statistic (CICc).[138,139]

To evaluate the sensitivity of the model to variations in taxonomic scale, and to assess whether our results are robust to ecological differences among clades, we repeated the analyses for two contrasting groups: passerine birds (order Passeriformes), representing small, land-based, and sedentary species, and a clade of largely aquatic birds including shorebirds, gulls, and terns (Charadriiformes), rails and cranes (Gruiformes), and a diverse array of aquatic and marine birds (Aequornithes).

Trait-dependent speciation and extinction

We analyzed how factors influenced lineage diversification rates using Quantitative State Speciation and Extinction (QuaSSE) models in the R package *diversitree* v.0.10-1[104] considering constant, linear, quadratic, sigmoidal, and unimodal effects of traits on diversification rates. For the linear model, we used the *make.linear.x* function to build a function in which diversification rates change linearly with changes in the trait value, except that rates are conditioned to always be positive (rates are set to zero any time the linear relationship suggest negative rates) and the relationships become constant outside the range of values of the trait (to match model assumptions[43]). The sigmoidal model assumes that rates at low and high values of the trait may be different (y_0 and y_1, respectively) and bridged by a sigmoidal function with parameter x_{mid} controlling the central location of the transition, and parameter r controlling the smoothness (steepness) of the transition.[43] We implemented a new quadratic mode in a function *make.quad.x*, in which diversification rates change with the trait values following a quadratic function, with the additional conditions of always positive values and constancy outside the range like in *diversitree*'s linear model. Finally, we implemented a new unimodal model in which rates peak at intermediate values of the trait using the formula:

$$y = h * e^{-\frac{(x-\mu)^2}{2\sigma^2}}$$

in which the multiplier h controls the height of the peak (the maximum rate), μ is the mean parameter controlling the position of the peak, and σ^2 is the variance parameter controlling the spread. This new function, *noroptimal2.x*, differs from the *noroptimal.x* function included in *diversitree* in lacking vertical offsets. which has the effect of lowering rates towards zero at extreme values of a trait. This allows testing of the intermediate dispersal model without additional offset parameters.

We fit four sets of models for each trait: 1) varying the model of trait dependence on speciation while holding extinction at zero (no-extinction models), 2) varying the model of trait dependence on speciation while holding extinction constant, 3) varying the model of trait dependence on extinction while maintaining speciation constant, and 4) varying the model of trait dependence on both

speciation and extinction. For the latter, we use the same function for speciation and extinction to reduce the number of models to be evaluated. We then used AIC and standard model selection techniques to identify the best models.[133,134]

Because QuaSSE models are prone to false positives,[45] we evaluated effects of traits on diversification using two alternative techniques that are more conservative. First, we used Hidden State Speciation and Extinction (HiSSE) models[44] on discretized versions of our continuous factors. Body mass, the Hand-wing index, and geographic range size were split at the median values, latitude was split into tropical versus extra-tropical (limit at 23.44 degrees). We fit two character-dependent diversification models, one with two observed states, only (BiSSE), and another with two observed and two hidden states (HiSSE). For comparison, we fit two Character Independent Diversification (CID) models, one with two hidden states (CID2) and another with four hidden states (CID4). For HiSSE and CID, we further evaluated models in which all state transition rates were equal (including hidden states) and models in which state transitions were unequal but symmetrical (e.g. rates 0 to 1 = rates 1 to 0). We fitted models by maximum likelihood with the *fit_musse* function in the R package *castor*[105] and defining trait type (observed or hidden), and state transition matrices following Beaulieu & O'Meara.[44] For geographic range size, we fit cladogenetic state-dependent diversification models in which ranges are reduced during speciation events using the method described by Smyčka et al.[39] based on functions in the *secsse* R package.[106] We compared models using the Akaike Information Criterion.[133]

Second, we used ES-sim, a semi-parametric method based on trait simulations to evaluated the statistical significance of a linear correlation between traits and species-specific speciation rate estimates.[45] We used our ClaDS estimates of species-specific speciation rates and fast Brownian motion rate estimation and simulation using functions *phylolm* and *rTrait* in the *phylolm* package.[102]

Current Biology, Volume *35*

Supplemental Information

A new time tree of birds reveals the interplay between dispersal, geographic range size, and diversification

Santiago Claramunt, Catherine Sheard, Joseph W. Brown, Gala Cortés-Ramírez, Joel Cracraft, Michelle M. Su, Brian C. Weeks, and Joseph A. Tobias

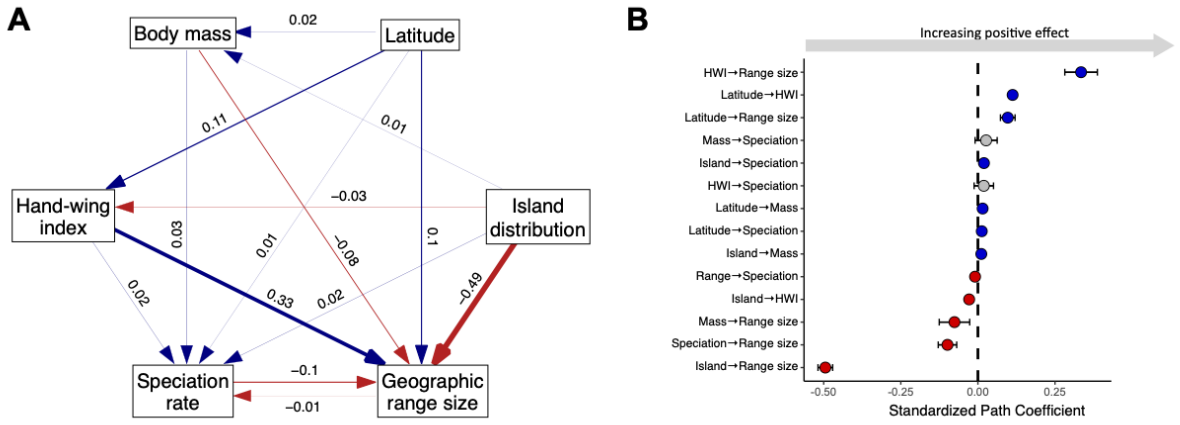

Figure S1. Phylogenetic path analysis of macroecological and macroevolutionary factors in birds using an alternative definition of island dwelling. Related to Figure 4.
Island distribution is defined as the proportion of the species' geographical distribution restricted to small islands (<2,000 km^2), with data from Sheard et al.[S1].
(A) Graph showing paths (arrows) and associated path coefficients representing the direction and strength of the effects of one factor onto another. Arrow thickness is proportional to the magnitude of the effect (path coefficient), and arrow color indicates the direction of the effect: positive (blue) or negative (red). Body mass, geographic range size, and speciation rates were log-transformed. Latitude refers to absolute latitude of the centroid of the species' geographical range.
(B) Standardized path coefficients with confidence intervals for each path. "HWI" is the Hand-wing Index. Dot color indicates the direction and statistical significance of the effect based on the confidence interval: positive (blue), negative (red), statistically not different from zero (gray).

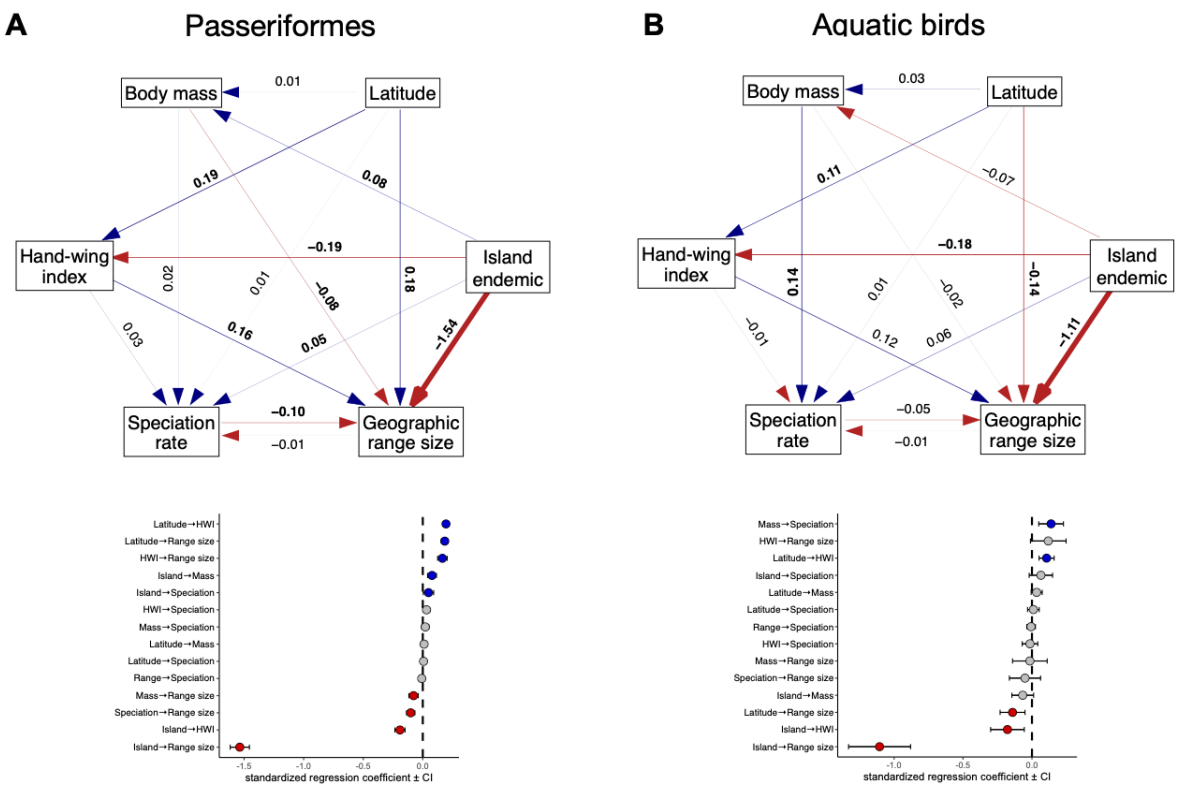

Figure S2. Phylogenetic path analysis of macroecological and macroevolutionary factors in two contrasting groups of birds. Related to Figure 4. (A) Path graph and corresponding for the order Passeriformes. (B) Path graph of aquatic birds including the Charadriiformes (shorebirds, gulls, and terns), Gruiformes (rails and cranes), and a Aequornithes (petrels, penguins, loons, herons, storks, ibises, cormorants, pelicans, and relatives). For both panels, the graph shows paths (arrows) and associated path coefficients representing the direction and strength of the effects of one factor onto another. Arrow thickness is proportional to the magnitude of the effect (path coefficient), and arrow color indicates the direction of the effect: positive (blue) or negative (red). Body mass, geographic range size, and speciation rates were log-transformed. Latitude refers to absolute latitude. Below each graph, standardized path coefficients are shown with confidence intervals for each path. The dot color indicates the direction and statistical significance of the effect based on the confidence interval: positive (blue), negative (red), statistically not different from zero (gray). HWI: Hand-wing Index.

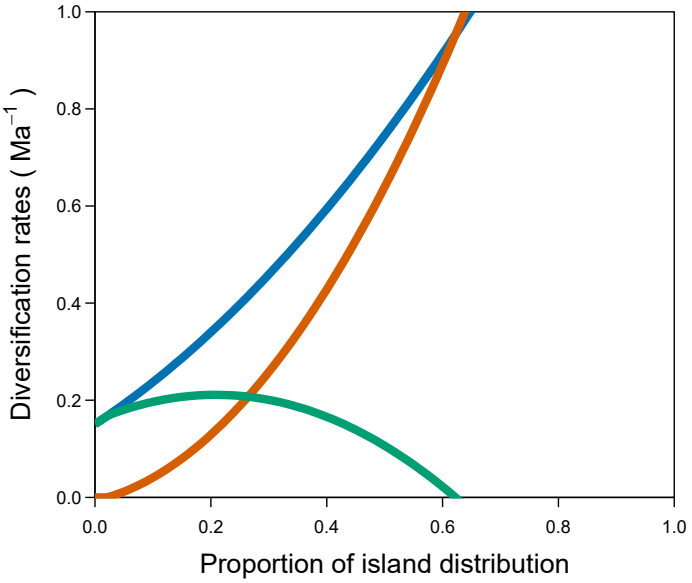

Figure S3. Effect of island dwelling on speciation and extinction rates using an alternative definition of island dwelling. Related to Figure 5. Lines show predictions from Quantitative-state Speciation and Extinction (QuaSSE) models in which both speciation rates (blue) and extinction rate (orange) change according to a quadratic function with respect to the proportion of island distribution. Also shown is the net diversification rate (green) calculated as speciation rate – extinction rate. The proportion of island distribution reflects the proportion of the geographical range restricted to small islands (<2,000 km^2), obtained from Sheard et al.[S1] (see Methods). The best model was identified using the same model selection techniques applied in the main analysis.

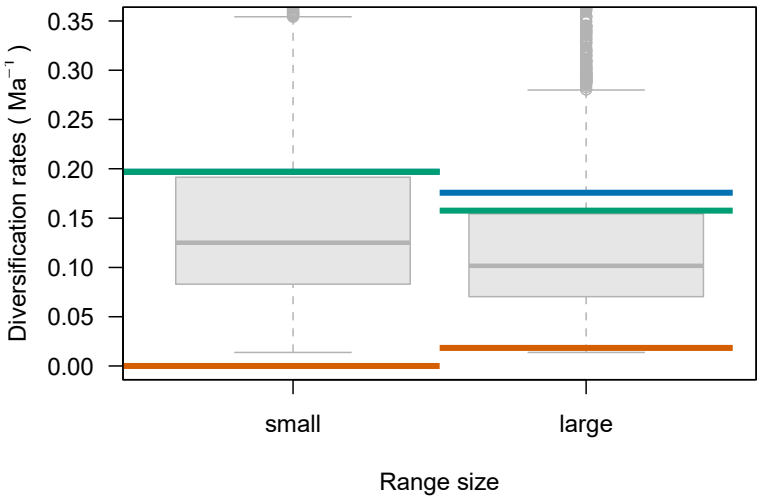

Figure S4. The influence of geographic range size on diversification rates. Related to Figure 5. Lines show diversification rate estimates from a Geographic Hidden-state Speciation and Extinction model in which geographic range size may decrease during speciation:[S2] speciation rates (blue), extinction rate (orange), and net diversification rate (green) calculated as speciation rate – extinction rate. The gray boxplot represents speciation rates estimated using the ClaDS method,[S3] shown for comparison.

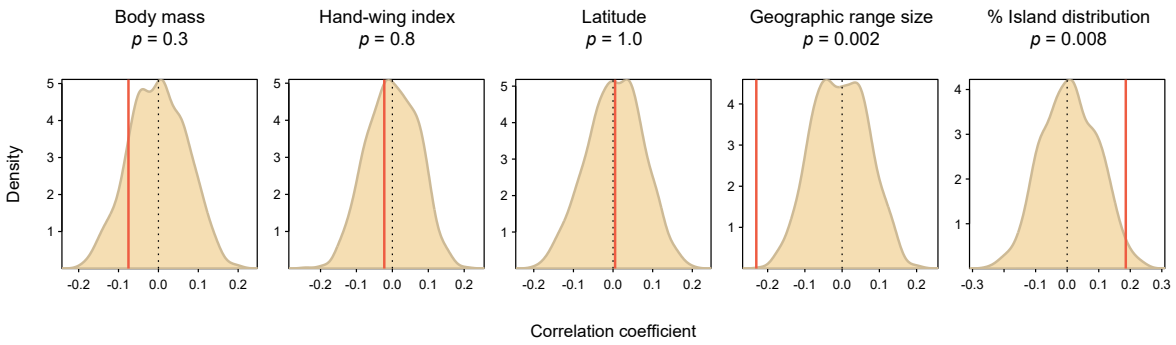

Figure S5. Evaluation of linear effects of traits on speciation rates (ClaDS estimates) using the ES-sim method. Related to Figure 5. Brownian rates and random traits simulations were obtained using functions *phylolm* and *rTrait* in the *phylolm* package.[S4] Body mass, and geographic range size were log-transformed. Latitude is the absolute value of latitude at the centroid of the species' geographical range. Speciation rates are significantly lower for large range sizes and significantly higher for birds in small islands.

Model	log(Lik)	AIC	ΔAIC	σ^2	α
log(**Body mass**)					
Lambda	-4138.3	8282.6	0	0.018	0.99
Kappa	-4270.3	8546.6	264.0	0.039	0.52
Ornstein–Uhlenbeck	-5590.9	11187.9	2905.3	0.037	0.01
Delta	-5621.7	11249.5	2966.9	0.013	2.70
Brownian motion	-5664.1	11332.2	3049.6	0.034	-
Early burst	-5664.1	11334.2	3051.6	0.034	0
Hand-wing index					
Lambda	-25228.4	50462.8	0	1.52	0.96
Kappa	-25650.7	51307.4	844.5	6.18	0.32
Ornstein–Uhlenbeck	-27794.9	55595.7	5132.9	6.89	0.03
Delta	-28032.3	56070.6	5607.8	2.01	3
Brownian motion	-28218.4	56440.7	5977.9	5.81	-
Early burst	-28218.4	56442.7	5979.9	5.81	0
abs(**Latitude**)					
Lambda	-33737.9	67481.8	0.0	7.1	0.91
Kappa	-34024.0	68054.1	572.2	48.0	0.17
Ornstein–Uhlenbeck	-35588.5	71183.0	3701.2	85.0	0.16
Delta	-37069.9	74145.7	6663.9	16.1	3
Brownian motion	-37331.1	74666.1	7184.3	47.3	-
Early burst	-37331.1	74668.1	7186.3	47.3	0
log(**Geographic range size**)					
Lambda	-20418.6	40843.2	0.0	0.15	0.69
Kappa	-21178.5	42363.1	1519.9	2.87	0.00
Ornstein–Uhlenbeck	-21900.1	43806.1	2962.9	8.81	0.47
Delta	-25774.2	51554.4	10711.2	1.22	3
Brownian motion	-26075.5	52155.1	11311.9	3.60	-
Early burst	-26075.5	52157.1	11313.9	3.60	0
log(**Speciation rate**)					
Kappa	1010.0	-2014.0	0.0	0.0179	0.00
Lambda	-658.1	1322.2	3336.2	0.0086	0.99
Ornstein–Uhlenbeck	-1296.3	2598.6	4612.6	0.0165	0.04
Delta	-1444.7	2895.4	4909.4	0.0047	3
Brownian motion	-1576.0	3156.0	5170.0	0.0133	-
Early burst	-1576.0	3158.0	5172.0	0.0133	0

Table S1. Results of trait evolution models. Related to STAR Methods. Six models of trait evolution were evaluated: Brownian motion (simple drift), *lambda* (phylogenetic signal), *delta* (time varying), Early burst (faster early trait evolution), Ornstein-Uhlenbeck (drift with an attractor), and *kappa* (speciational change). Reported statistics are the log-likelihood (log(lik)), Akaike Information Criterion (AIC), differences in AIC respect to the best model (ΔAIC), the Brownian rate (σ^2), and the additional parameters of the different models (α). Models were estimated using intercept-only models with the function *phylolm*[S4] in R, the newly assembled time-tree of birds, and trait information from the AVONET database.[S5]

Path Coefficients						
	Island	Latitude	Mass	HWI	Speciation	Range size
Island	0	0	0.014	-0.116	0.045	-1.483
Latitude	0	0	0.021	0.110	0.010	0.125
Mass	0	0	0	0	0.031	-0.073
HWI	0	0	0	0	0.032	0.235
Speciation rate	0	0	0	0	0	-0.122
Range size	0	0	0	0	-0.009	0

Lower bound						
	Island	Latitude	Mass	HWI	Speciation	Range size
Island	0	0	-0.003	-0.136	0.014	-1.546
Latitude	0	0	0.014	0.102	-0.002	0.103
Mass	0	0	0	0	-0.004	-0.119
HWI	0	0	0	0	0.002	0.183
Speciation rate	0	0	0	0	0	-0.150
Range size	0	0	0	0	-0.018	0

Upper bound						
	Island	Latitude	Mass	HWI	Speciation	Range size
Island	0	0	0.031	-0.096	0.076	-1.420
Latitude	0	0	0.027	0.118	0.021	0.148
Mass	0	0	0	0	0.066	-0.026
HWI	0	0	0	0	0.062	0.286
Speciation rate	0	0	0	0	0	-0.095
Range size	0	0	0	0	0.000	0

Table S2. Results of path analyses. Related to Figure 4. Coefficient estimates, and lower and upper bounds, from a phylogenetic path analysis[S6] of the interrelationships among dispersal proxies, geographic covariates, and speciation rates in the world's birds. Island is a binary factor indicating whether the species is an island endemic or not based on Sayol et al.;[S7] Latitude is the absolute latitude of the centroid of the species' geographical range; Mass is the logarithm of total body mass; HWI is the Hand-wing Index; Speciation rate is the speciation rate estimated using the ClaDS method;[S3] Range size is the logarithm of the geographic range size.

Speciation	Extinction	log(Lik)	k	AIC	ΔAIC
Linear	linear	-27910.3	5	55830.7	0
Constant	sigmoid	-27910.7	6	55833.5	2.8
Sigmoid	sigmoid	-27915.5	9	55849.1	18.4
unimodal	unimodal	-27922.0	7	55858.0	27.3
constant	unimodal	-27928.0	5	55866.0	35.3
sigmoid	constant	-27971.9	6	55955.8	125.1
quadratic	quadratic	-27992.8	7	55999.6	168.9
linear	constant	-27996.4	4	56000.9	170.2
quadratic	constant	-27996.5	5	56003.0	172.3
unimodal	constant	-27997.2	5	56004.5	173.8
constant	quadratic	-28061.9	5	56133.7	303.0
constant	constant	-28065.7	3	56137.3	306.6
constant	linear	-28067.3	4	56142.5	311.9

Table S3. Quantitative State Speciation and Extinction models of the effect of body mass (log-transformed) on diversification rates. Related to Figure 5. Models were estimated using a global time-tree of birds. Reported statistics are the log-likelihood (log(lik)), number of parameters (k), Akaike Information Criterion (AIC), and differences in AIC compared to the best model (ΔAIC).

Speciation	Extinction	log(Lik.)	k	AIC	ΔAIC
constant	sigmoid	-48902.7	6	97817.5	0
sigmoid	sigmoid	-48926.0	9	97870.0	52.5
constant	quadratic	-48952.9	5	97915.8	98.3
sigmoid	constant	-48963.7	6	97939.4	121.9
linear	linear	-48971.0	5	97952.1	134.6
quadratic	quadratic	-48978.7	7	97971.3	153.8
constant	linear	-48986.5	4	97981.0	163.5
constant	unimodal	-48988.4	5	97986.7	169.2
linear	constant	-48993.6	4	97995.1	177.7
quadratic	constant	-48995.0	5	98000.0	182.6
constant	constant	-49005.6	3	98017.2	199.7
unimodal	unimodal	-49006.2	7	98026.4	208.9
unimodal	constant	-49029.9	5	98069.9	252.4

Table S4. Quantitative State Speciation and Extinction models of the effect of the Hand-wing index on diversification rates. Related to Figure 5. Models were estimated using a global time-tree of birds. Reported statistics are the log-likelihood (log(lik)), number of parameters (k), Akaike Information Criterion (AIC), and differences in AIC compared to the best model (ΔAIC).

Speciation	Extinction	log(Lik.)	k	AIC	ΔAIC
constant	linear	-58320.3	4	116648.7	0
linear	linear	-58339.9	5	116689.8	41.1
unimodal	unimodal	-58872.6	7	117759.1	1110.4
sigmoid	sigmoid	-58980.7	9	117979.4	1330.7
constant	sigmoid	-59022.4	6	118056.8	1408.1
quadratic	constant	-59189.9	5	118389.8	1741.1
sigmoid	constant	-59210.0	6	118432.0	1783.3
quadratic	quadratic	-59264.6	7	118543.1	1894.4
unimodal	constant	-59581.7	5	119173.5	2524.8
linear	constant	-59713.0	4	119434.0	2785.3
constant	constant	-59794.1	3	119594.3	2945.6
constant	quadratic	-59799.9	5	119609.8	2961.1
constant	unimodal	-59801.6	5	119613.1	2964.4

Table S5. Quantitative State Speciation and Extinction models of the effect of absolute latitude on diversification rates. Related to Figure 5. Models were estimated using a global time-tree of birds. Reported statistics are the log-likelihood (log(lik)), number of parameters (k), Akaike Information Criterion (AIC), and differences in AIC compared to the best model (ΔAIC).

Speciation	Extinction	log(Lik.)	k	AIC	ΔAIC
sigmoid	sigmoid	-45814.6	9	91647.3	0
unimodal	unimodal	-46600.3	7	93214.7	1567.4
sigmoid	constant	-46639.9	6	93291.8	1644.5
quadratic	constant	-46692.3	5	93394.5	1747.2
linear	constant	-46836.2	4	93680.3	2033.0
quadratic	quadratic	-46890.4	7	93794.8	2147.5
constant	quadratic	-46945.3	5	93900.7	2253.4
unimodal	constant	-47199.4	5	94408.8	2761.5
linear	linear	-47243.3	5	94496.7	2849.4
constant	linear	-47282.3	4	94572.6	2925.3
constant	constant	-47359.3	3	94724.6	3077.3
constant	sigmoid	-47358.2	6	94728.4	3081.1
constant	unimodal	-48203.2	5	96416.4	4769.1

Table S6. Quantitative State Speciation and Extinction models of the effect of geographic range size on diversification rates. Related to Figure 5. Models were estimated using a global time-tree of birds. Reported statistics are the log-likelihood (log(lik)), number of parameters (k), Akaike Information Criterion (AIC), and differences in AIC compared to the best model (ΔAIC).

Model	observed	hidden	log(Lik.)	AIC	ΔAIC
Mass					
ClD4sym	0	4	-26783.7	53615.3	0.0
ClD4er	0	4	-27157.1	54332.2	716.8
ClD2sym	0	2	-27329.3	54674.6	1059.3
HiSSEer	2	2	-27366.1	54750.2	1134.8
ClD2er	0	2	-27402.0	54813.9	1198.6
BISSE	2	0	-27874.3	55760.6	2145.3
HiSSEsym	2	2	-28224.4	56472.7	2857.4
HWI					
ClD2sym	0	2	-28364.6	56745.3	0.0
ClD4sym	0	4	-28350.6	56749.2	4.0
ClD4er	0	4	-28611.9	57241.9	496.6
BiSSE	2	0	-28779.1	57570.1	824.8
HiSSEsym	2	2	-28989.1	58002.1	1256.9
HiSSEer	2	2	-29428.1	58874.2	2129.0
ClD2er	0	2	-29944.1	59898.2	3153.0
Latitude					
ClD2sym	0	2	-29533.4	59082.8	0.0
ClD2er	0	2	-29581.1	59172.1	89.3
BISSE	2	0	-30154.5	60321.0	1238.2
ClD4sym	0	4	-30266.6	60581.3	1498.5
HiSSEer	2	2	-30572.0	61161.9	2079.1
HiSSEsym	2	2	-30838.7	61701.3	2618.5
ClD4er	0	4	-30934.6	61887.2	2804.3
Island					
HiSSEer	2	2	-30360.0	60738.0	0.0
HiSSEsym	2	2	-30364.6	60753.2	15.2
BISSE	2	0	-30515.7	61043.4	305.3
ClD4er	0	4	-31042.9	62103.8	1365.8
ClD2er	0	2	-31417.5	62845.1	2107.1
ClD4sym	0	4	-32189.8	64427.6	3689.6
ClD2sym	0	2	-37213.7	74443.4	13705.4
Range size					
Smyčka III	2	2	-30151.6	60327.26	0.0
Smyčka IV	0	4	-30213.1	60466.24	139.0
Smyčka II	0	2	-30357.2	60726.38	399.1
Smyčka I	2	0	-31387.7	62785.42	2458.2

Table S7. Hidden State Speciation and Extinction models of the effect of dispersal proxies and geographic features on diversification rates when modeled as discrete (binary) traits. Related to Figure 5 and Figure S2. Reported statistics are the log-likelihood (log(lik)), Akaike Information Criterion (AIC), and differences in AIC compared to the best model (ΔAIC), and models a ordered from the best (ΔAIC = 0) to the worst. Body mass, Hand-wing index, and geographic range size were discretized based on values below or above the median value. Latitude was divided between tropical and extra tropical

latitudes (boundary: 23.44 degrees). Island dwelling was based on a list of species endemic to islands.[S7] Model differ in the number of "observed" and "hidden" states, with models including only hidden states representing character-independent model (CID) in which there is no effect of the observed trait on speciation and extinction. Models also differ in their state transition matrix, in which transition rates can be all equal (ER) or unequal but symmetrical (Sym). For geographic range size, we used a cladogenetic state-dependent diversification model in which range size changes during speciation (Smyčka et al.[S2]). See Methods for further details. Support for models that include "observed" states, indicate effects of the corresponding trait on diversification rates (Island, Range size).

Supplemental references

S1. Sheard, C., Neate-Clegg, M.H.C., Alioravainen, N., Jones, S.E.I., Vincent, C., MacGregor, H.E.A., Bregman, T.P., Claramunt, S., and Tobias, J.A. (2020). Ecological drivers of global gradients in avian dispersal inferred from wing morphology. Nat. Comm. *11*, 2463. https://doi.org/10.1038/s41467-020-16313-6.

S2. Smyčka, J., Toszogyova, A., Storch, D. (2023). The relationship between geographic range size and rates of species diversification. Nat. Comm. *14*, 5559. https://doi.org/10.1038/s41467-023-41225-6.

S3. Maliet, O., and Morlon, H. (2022). Fast and accurate estimation of species-specific diversification rates using data augmentation. Syst. Biol. *71*, 353–366. https://doi.org/10.1093/sysbio/syab055.

S4. Tung Ho, L. si, and Ané, C. (2014). A linear-time algorithm for Gaussian and non-Gaussian trait evolution models. Syst. Biol. *63*, 397–408. https://doi.org/10.1093/sysbio/syu005.

S5. Tobias, J.A., Sheard, C., Pigot, A.L., Devenish, A.J.M., Yang, J., Sayol, F., Neate-Clegg, M.H.C., Alioravainen, N., Weeks, T.L., Barber, R.A., et al. (2022). AVONET: morphological, ecological and geographical data for all birds. Ecol. Lett. *25*, 581-597. https://doi.org/10.1111/ele.13898.

S6. von Hardenberg, A., Gonzalez-Voyer, A. (2013). Disentangling evolutionary cause-effect relationships with phylogenetic confirmatory path analysis. Evolution *67*, 378-387. https://doi.org/10.1111/j.1558-5646.2012.01790.x.

S7. Sayol, F., Steinbauer, M.J., Blackburn, T.M., Antonelli, A., Faurby, S. (2020). Anthropogenic extinctions conceal widespread evolution of flightlessness in birds. Science Advances *6*, eabb6095. https://doi.org/10.1126/sciadv.abb6095.